

DEPARTMENT OF THE INTERIOR

U.S. GEOLOGICAL SURVEY

Tephrochronologic studies of sediment cores from Walker Lake, Nevada

by

Andrei M. Sarna-Wojcicki¹, Kenneth R. Lajoie¹, Charles E. Meyer¹,
David P. Adam¹, Steven W. Robinson¹, and R. Scott Anderson²

Open-File Report 88-548

This report is preliminary and has not been reviewed for conformity with U.S. Geological Survey editorial standards and stratigraphic nomenclature. Any use of trade names is for descriptive purposes only and does not imply endorsement by the USGS.

¹U.S. Geological Survey, 345 Middlefield Road, Menlo Park, CA 94025

²Department of Geology, University of Arizona, Tucson, AZ 85721

1988

Table of Contents

Introduction	3
Summary	4
Methods	4
Results	6
Upper Holocene tephra layers of Walker Lake	6
Discussion of ages of upper Holocene tephra layers in Walker Lake	10
Tephra layers at intermediate depths in the deeper Walker Lake cores, near the base of core WLC84-2 and 3, and in core WLC85-2	11
Discussion of correlations of tephra layers at intermediate depths in the deeper Walker Lake cores	14
Ages of the lowermost tephra layers in the deeper Walker Lake cores ..	14
Summary and Discussion	15
Acknowledgements	20
References	21

List of Figures

- Figure 1. Sites in the western United States and eastern Pacific Ocean where age control for sediments of Walker Lake is obtained by tephra correlations.
- Figure 2. Locations of sediment cores in Walker Lake
- Figure 3. Locations of cores and exposures south of Walker Lake where tephra layers are found that correlate with those in Walker Lake
- Figure 4. Graphic logs of upper Holocene tephra in Walker Lake cores, the Crooked Meadow section, and Barrett Lake
- Figure 5. Graphic logs of Holocene and upper Pleistocene tephra layers in Walker Lake cores
- Figure 6. Sedimentation-rate curves for upper Holocene sediments in Walker Lake, Crooked Meadow, and Barrett Lake
- Figure 7. Sedimentation-rate curves for Walker Lake cores WLC75-B, -D, and -E, WLC76-G, and WLC84-8
- Figure 8. Ages of upper Holocene tephra layers and zones of disseminated glass shards in Walker Lake core WLC84-8, the Crooked Meadow section, and the Barrett Lake core
- Figure 9. Correlation chart for tephra layers in Walker Lake cores and tephra layers at some sites in the western conterminous United States and northeastern Pacific Ocean
- Figure 10. Sedimentation-rate curve for the upper 40 m of sediments in Walker Lake, near the current depositional center
- Figure 11. Age vs. depth curve for the upper Quaternary sediments in the deep cores in Walker Lake, near the current depositional center

List of Tables

- Table 1. Electron-microprobe analysis of tephra from Walker lake and related tephra from other sites
- Table 2. Ages of young tephra layers in cores from Walker Lake, Crooked Meadow, and Barrett Lake
- Table 3. Radiocarbon ages used in estimating ages of tephra layers in Walker Lake
- Table 4-6. Electron-microprobe, X-ray fluorescence, and neutron-activation analyses of Quaternary tephra layers from Walker Lake and several other sites in the western conterminous United States

Introduction

Studies of cores from Walker Lake were conducted to determine the nature of climatic changes in mid- to late-Quaternary time in the southwestern Great Basin (Benson, 1988). Our contribution to this effort is a tephrochronologic study to help provide a numerical chronology for the paleoclimatic studies.

The upper several tens of meters of the Walker Lake cores are dated by radiocarbon (Benson, 1988; Yang, 1988). Sediments lower in the cores are beyond the range (ca. 35-40 Ka) of conventional radiocarbon dating. Tephrochronology, together with other techniques such as amino-acid racemization and uranium-series analyses, can provide age control for the lower part of the cored sections, and independent checks for the upper parts of cores dated by radiocarbon analyses.

Our studies consisted of (1) examination of sediments of Walker Lake cores for presence of tephra layers or zones of disseminated volcanic glass shards, (2) sampling of the sediments for tephra, (3) petrographic analysis of tephra samples, (4) separation of volcanic glass from the samples, (5) chemical analysis of the volcanic glass shards by electron-microprobe (and, for some samples, energy-dispersive X-ray fluorescence and neutron-activation) analyses and (6) correlation of tephra layers from Walker Lake cores with tephra layers from other independently dated stratigraphic sections within conterminous North America, using chemical and petrographic criteria. With the exception of some of the late Holocene tephra layers near the top of the lake sediments, ages of tephra layers in Walker Lake are thus determined by correlation, rather than by direct age analyses of sediments in the cores.

Localities from which tephrochronologic and tephrostratigraphic information was obtained during this study are shown in figures 1-3. We have analyzed samples from the following cores in Walker Lake: WLC75-E, WLC76-G, WLC84-2, 3, 4, 5, 8, and WLC85-2 (fig. 2). Initially, samples from all discrete tephra layers from these cores were analyzed by electron microprobe (EM) (figs. 4, 5; table 1). Subsequently, we analyzed glass shards from a number of additional zones of disseminated glass shards identified in the cores by William Thordarson (U.S.G.S, Denver) using smear slides. Most of these samples had a very small percentage of glass shards, and were probably from older tephra layers. In most cases, these samples probably represent an "ambient" content of reworked tephra within the sediments that contain them. This observation is strengthened by the fact that the chemical composition of tephra shards from these samples are usually heterogeneous, and thus are mixtures of several tephra layers. Some of the disseminated shards from these samples, however, are chemically homogeneous, and thus probably correspond quite accurately to the original time/stratigraphic positions of the parent tephra layers.

Results of our chemical analyses have been compared with our current EM data base of tephra layers from conterminous North America, and correlations have been determined primarily by computer analysis of the chemical data. Concurrently, we have also conducted energy-dispersive X-ray fluorescence (XRF) and instrumental neutron activation (INA) analyses on some samples to determine new correlations and to test correlations we have made on the basis of EM data. This has been done only on the thicker tephra layers obtained from the cores, because XRF and INA require bulk separates of about 0.5 g of

pure glass. A considerably larger initial amount of raw material is needed to obtain 0.5 g of glass.

Summary

Our tephra correlations, together with biostratigraphy and radiocarbon ages on the Holocene tephra layers, indicate that: 1) a 3-to-4-cm thick tephra layer that is widespread near the top of the sediments in Walker Lake, at depths of several tens of centimeters to about 3.2 m, is about 1200-yr. b.p. (assuming that there is little or no reservoir effect in the radiocarbon analyses), and equivalent to Wood's (1977) tephra 2; 2) tephra layers at depths of about 20 to 21 m in WLC84-2, at 32 to 44 m in WLC84-4, and at about 37 m in WLC84-5 correlate with tephra layers in the lower part of the Wilson Creek beds, in Mono Lake basin, Ca., and are thus about 28-36 Ka in age; 3) the tephra layer at 21.02 m in WLC84-2 may correlate with a tephra layer at a depth of about 65 m in cores WLC84-4 and WLC84-5; this is probably the case only if a hiatus is present between 20.77 and 21.02 m in WLC84-2; 4) the tephra layers at intermediate depths of about 65 to 79 m in WLC84-4 and WLC84-5 are in the age range of about 50 to 150 Ka b.p., based on correlations to the Negit Causeway in Mono Lake basin and, in turn, to volcanic units at Mammoth Mountain in the Long Valley caldera, Ca.; 5) tephra layers near the base of the deeper Walker Lake cores WLC84-4 and WLC84-5, at about 142-146 m (fig. 5), are probably about 300 to 370 Ka, based on correlations to Paoha Island in Mono Lake, Benton Crossing in Long Valley caldera, Ca., Tulalake, Ca., and Summer Lake, Ore.; and 6) sediments at the bottom of these deeper cores (ca. 150 m) are not older than about 400 Ka.

Methods

We disaggregated and sieved tephra samples using nylon screens and plastic holders to avoid contamination with metals, and separated glass and phenocrysts using solutions of methylene iodide and acetone, and magnetic separators (Sarna-Wojcicki, 1976; Sarna-Wojcicki and others, 1979; 1984). We analyze glass shards to determine correlations among tephra layers because the volcanic glass is usually the most homogenous phase, and is generally the most distinctive for chemical characterization of tephra. Glass samples were analyzed by EM using a 9-channel SEMQ electron microprobe (located at the U.S. Geological Survey, Menlo Park) for 9 major and minor oxides: SiO_2 , Al_2O_3 , Fe_2O_3 , MgO , MnO , CaO , TiO_2 , Na_2O , and K_2O (Sarna-Wojcicki and others, 1984). For purposes of comparison, we selected oxides on the basis of their natural variability within and between tephra layers, as well as according to precisions attainable for each oxide by EM analysis. For rhyolitic glasses of mid- to late-Quaternary age, the oxides present in the highest concentrations, SiO_2 , Al_2O_3 , Fe_2O_3 , CaO , Na_2O , and K_2O , discriminate best among tephra layers. In rhyolitic glasses, MgO , MnO , and TiO_2 generally occur in concentrations that are close to the detection limit by EM analysis, and thus analyses for these are imprecise and not useful for quantitative comparisons, although they are still useful for qualitative evaluation of the data. More basic glasses generally contain higher concentrations of MgO , TiO_2 , and sometimes MnO , consequently analyses for these oxides can be often used as well in quantitative comparisons of more basic tephra.

The totals of oxides for most analyses of volcanic glass are less than 100 percent owing to the presence of water and other volatile fluids, as well

as minor elements that are not detected by EM analysis. Oxides in glasses of youngest silicic tephra layers (0 to 4 Ka) usually total 97 to 99 percent; oxides in glasses of older silicic tephra generally total less--90 to 97 percent, because natural glass hydrates with time. The oxides in less silicic glasses tend to have higher totals than more silicic glasses of the same age. For purposes of comparison, we recalculated oxide concentrations to 100 percent because the resultant values tend to be less scattered for glasses of the same tephra layers obtained from different depositional environments. The original totals are given in table 1; the original analyzed values of each oxide concentration can be recalculated from these totals.

Chemical compositions of glass samples were matched using the similarity coefficient (SIMANAL) (Borchardt and others, 1972; Sarna-Wojcicki, 1976; Sarna-Wojcicki and others, 1979; 1984). This coefficient varies between 0 and 1, where 1 represents identity (a perfect match). Similarity coefficients for replicate analyses of samples from a single tephra layer in EM analysis generally range between 0.96 and 0.99, and between about 0.94 and 0.99 in XRF and INA analyses, depending on the elements used, their concentrations in the glasses, and the chemical characteristics of the tephra units analyzed. Similarity coefficients between tephra layers of demonstrably different age usually are lower. Some tephra layers erupted from the same volcano or volcanic province are very similar in glass chemical composition, and cannot be distinguished on the basis of EM analysis (similarity coefficients are in the range of 0.95 to 0.98). If samples from such tephra layers are large enough to obtain a sufficient quantity of pure glass, then it is usually possible to distinguish between them by XRF or INA analyses. Tephra samples from cores are often too small to obtain a sufficient amount of glass for XRF or INA analyses, thus only a few core samples of tephra layers from Walker Lake were analyzed by the latter methods.

The similarity coefficient makes it possible to evaluate a large number of samples for many variables, and to select those samples which are most similar. The latter group of samples are then evaluated further to determine the nature of the distribution of each variable (for instance, as to whether is it narrow, scattered, or polymodal), and for stratigraphic position and other independent age information associated with each sample in the group. Those samples that are the most similar with respect to all the observable criteria, and that fall within the limits of replication of individual tephra layers, are identified as possible correlatives.

We have the greatest confidence in correlations where we can document the existence of characteristic stratigraphic sequences of several tephra layers (in terms of the chemical compositions and petrography of the tephra layers and their relative stratigraphic position to other layers) at two or more localities. This is because the probability that the occurrence of a particular characteristic sequence at two localities is due to chance decreases with the number of layers in the sequence. Thus, for four tephra layers that occur within a stratigraphic sequence and that can be distinguished from each other by physical or chemical properties, the probability of another stratigraphic sequence of four tephra layers occurring in the same order due to chance alone is equal to one divided by factorial four, or four percent. This probability decreases further with increasing number of tephra layers in a sequence. The only reasonable alternative to chance for the occurrence of such tephra sequences is that the sequences are

correlative in time, because although recurrent cyclic patterns of eruption through time can occur, such cycles are never so regular as to produce an exact replication of a multi-tephra sequences at two different times. Such a replication would be even less likely for a sequence of tephra layers erupted from more than one source area, because it would require coordinated timing of eruptions of tephra among eruptive sources.

Results

The stratigraphic positions of tephra layers and zones of disseminated volcanic glass shards from cores of Walker Lake sediments analyzed by EMA are shown in figures 4 and 5. Figure 4 shows the positions of analyzed samples from the upper 12 m of the Walker Lake cores (WLC75-E, WLC84-8, and WLC76-G), and from stratigraphic sections that contain tephra layers of about the same age at Crooked Meadow and Barrett Lake. Figure 5 shows the stratigraphic position of tephra layers and zones of disseminated glass shards analyzed from the deeper Walker Lake sediments (cores WLC84-2 through -5). Results of EM analysis of tephra layers and disseminated shards in cores obtained from Walker Lake are given in table 1. Additional analyses by XRF and INA are given in tables 4 through 6. Tentative correlations of upper Holocene tephra layers and disseminated zones of glass shards between cores in Walker Lake and other sites in the study area are shown in figure 4. Correlations among tephra layers from intermediate to deep levels in Walker Lake cores, and to tephra layers at other sites in the western U.S., are shown in figure 9.

Upper Holocene tephra layers of Walker Lake

Most of the tephra layers in the uppermost 12 m of sediment in Walker Lake (WLC75-E, WLC76-G, WLC84-2, -4, and -8; figs. 4 and 5) were erupted from the Mono Craters volcanic center, located about 100 km south of Walker Lake (fig. 3), as indicated by the chemical similarity of these layers to thick, coarse Holocene tephra sequences at, and in the immediate vicinity of, the Mono Craters (table 1). One tephra layer, however, was erupted from the Inyo Craters, located to the south of the Mono Craters (fig. 3; table 1). The chemical compositions and petrographic characteristics of late Holocene tephra layers erupted from the Mono Craters are very similar, and it is difficult or impossible to distinguish among them on the basis of EM analysis and petrographic characteristics. Those tephra layers that are in closest stratigraphic proximity appear to be the most similar, suggesting that chemical differentiation is the mechanism by which the composition of tephra from this source changes with time, and that a large magma reservoir is being tapped to produce the tephra of these layers. Otherwise we would expect successive tephra layers from this source to show greater differences in chemical composition. These young tephra layers can, however, be partially distinguished by using a combination of criteria including thickness, depth, stratigraphic sequence, stratigraphic relationships to ecostratigraphic events, radiocarbon ages, and chemical composition. These criteria have been used to distinguish two sets of late Holocene tephra in Walker Lake that were erupted during two recent episodes of volcanic activity at the Mono Craters. If there is no appreciable carbon reservoir effect in Walker Lake due to the presence of old dissolved carbonate, the older set is about 4600 to 3500 yr b.p., and the younger set, about 2500 to about 900 yr. b.p. (ages based on radiocarbon dates on organic materials from the Walker Lake cores; Benson, 1988; Yang, 1988). Sets of tephra layers erupted from Mono Craters having

similar ages to those in Walker Lake are found at Crooked Meadow, 10 km east of the Mono Craters, and in Barrett Lake near Mammoth, Calif., 40 km south of the Mono Craters (figs. 3 and 4).

The ages of the layers in the younger set, estimated by interpolation from a sedimentation-rate curve derived from radiocarbon ages (uncorrected for secular ^{14}C variation) on organic material in core WLC-8 (Benson, 1988; Yang, 1988; fig. 6), are 920 yr. (2.18 m^{1/}), 1190 (2.67 m), 1300 (2.95-3.04 m^{2/}), and 1800 (3.67 m) yr. b.p. (table 2). Stratigraphic intervals containing zones of disseminated shards belonging to this younger set are estimated to be 430 yr. b.p. (0.93 m), 900 yr. (2.04 m), 1040 yr. (2.34 m), 1570 yr. (3.27 m), 1680 yr. (3.46 m), and 2100 yr. b.p. (4.09 m)(table 2). The only macroscopic tephra layer in the older set is estimated to be 4650 yr. b.p. (10.15 m), with disseminated zones of tephra at 3840 yr. (7.98 m), 4230 yr. (8.99 m), and 4500 yr. b.p. (9.70 m)(table 2). The radiocarbon ages used for these estimates are on organic material, rather than on carbonate, in order to minimize a possible reservoir effect of unknown magnitude. In all instances except one, ages on the organic material in WLC84-8 were younger than on carbonate, suggesting that a reservoir effect for inorganic carbon does exist in Walker Lake. In the one instance where this relationship is reversed, we used an average of the ages determined on both organic material and carbonate (fig. 6), for lack of a better choice. The radiocarbon dates used in age estimates of the tephra layers are given in table 3, together with recalculated ages using the secular ^{14}C variation curve derived from dendrochronology (Stuiver and Reimer, 1986; Stuiver and Becker, 1986). Tephra layers in core WLC84-4 at 3.29 m and 3.31 m are probably from the same tephra layer and probably belong to the younger (ca. 900-2500-yr-b.p.) set of tephra layers found in core WLC84-8, based on depth in the core (fig. 5) and glass chemistry of these layers as determined by EM analysis (table 1). These uppermost tephra layers in core WLC84-4 are disturbed and somewhat deeper than in the nearby core WLC84-8, consequently they may have been translocated downward during coring.

There is also a layer of tephra about 2 cm thick in segment 2A of core WLC84-8, at a depth of 2.52 m, that was erupted from the Inyo Craters; this unit has an interpolated age of about 1150 yr b.p. on the basis of radiocarbon ages (uncorrected) in core WLC84-8. The base of this layer is about 6 cm above the top of the 5-cm-thick Mono Craters tephra layer at 2.67 m (fig. 4). The same two tephra layers are present in segment 3A of core WLC84-8, in the same sequence, and are separated by about the same thickness (7.5 cm) of lake sediments (fig. 4; table 1). These identifications support J. P. Bradbury's observation (written commun., 1985) that segment 3A of core WLC84-8 was displaced downward during coring by a malfunction of the coring mechanism.

On the basis of EM analysis, we correlate the Mono Craters tephra layer at 2.67 m in Walker core WLC-8 (table 1) with similar tephra layers in several Walker Lake cores on the basis of thickness and close stratigraphic position below the top of the Stephanodiscus niagarae interval (Bradbury, 1987). It is generally the thickest of the younger tephra layers in the Walker Lake cores (with the exception of the ash at 2.17 m in WLC8, segment 3A (14.5-20 cm)), and underlies the top of the S. niagarae zone by a more-or-less consistent

^{1/}Depths of tephra layers cited in this report are to the base of each layer.
^{2/}A deformed tephra layers that is at a 45-degree angle in the core.

stratigraphic thickness (figs. 4, 7). The interval containing S. niagarae probably represents a low salinity period in the lake, and the appearance of S. niagarae within a short stratigraphic interval is probably due to a rapid influx of fresh water into the lake (Bradbury, 1987), and as such is likely to be a nearly synchronous event throughout the lake. Using the radiocarbon age control in Walker Lake cores WLC75-B, D, E, and WLC84-8 (fig. 7, a-c, e; Bradbury, 1987), we estimate the age of the top of the S. niagarae zone to be 980 ± 90 yr b.p. (average of four values), and the age of the thick, ubiquitous Mono Craters tephra layer (at 2.69 m in WLC84-8, segment 2A, at 28.5-33 cm), to be 1130 ± 100 yr b.p. (average of four values). An estimate from Walker Lake core 8 alone yields an age of 1190 yr b.p. for this layer. These estimated ages are very close or the same as the 1190 ± 80 -yr-b.p. radiocarbon date of a widespread tephra layer erupted from the Mono Craters and found in mountain lakes and meadows at many localities in the east-central Sierra Nevada (tephra 2 of Wood, 1977). Barring the existence of a significant reservoir effect in Walker Lake due to the presence of dissolved old carbon in the lake water, we thus consider this layer (2.69 m in WLC84-8) to be correlative with Wood's tephra layer 2.

Sieh and Bursik (in press) have studied the areal distribution and stratigraphy of the youngest tephra layer produced by an eruption of the Mono Craters. They have determined its age by radiocarbon analyses to be 1395 ± 50 yrs. A.D. (or 555 yr b.p.; average of three dates, corrected for past secular variation of ^{14}C). Sieh and Bursik indicate that this layer is present to the north of Walker Lake, where they report its thickness to be 3.4 cm (their fig. 4). Their isopach map indicates that this layer should be about 4 to 5 cm thick within Walker Lake. However, our age and stratigraphic data indicate there is no layer having this thickness and age in the Walker Lake cores. Our data indicate that the thickest and most widely distributed of the upper Holocene ash beds in Walker Lake is about 1200 yr b.p., and that it underlies the top of the S. niagarae interval dated at about 980 yr b.p., as interpolated from radiocarbon ages. The age of Wood's tephra layer 2, dated at 1190 ± 80 (Wood, 1977), recalculates to 829 ± 98 AD when corrected for past secular variation of ^{14}C production in the atmosphere (Stuiver and Becker, 1986). The ^{14}C age determined by Sieh and Bursik on the youngest tephra layer erupted from the Mono Craters is significantly different from that of tephra layer 2 of Wood and its presumed correlative layer in Walker Lake at the 99 percent confidence level, and is thus unlikely to be the same unit unless the radiocarbon ages are in error. We estimate the age of the only thick (5.5 cm) Mono Craters ash bed above the top of the S. niagarae interval (WLC84-8-3A, 14.5-20 cm, at a depth of 2.17 m; figs. 4, 6, 7; tables 1 and 2) to be about 950 yr b.p. (about 920 b.p., when the ^{14}C dates are corrected). This ash closely overlies the S. niagarae interval by 8 cm; radiocarbon ages from other cores above this zone (fig. 7, a-c) do not indicate the presence of any hiatus above the ca. 1200-yr-b.p. ash bed or above the S. niagarae interval that would allow a younger age for this layer. We conclude that either (1) the ca. 555-yr-b.p. layer from Mono Craters is not present in Walker Lake, or (2) that the 5.5-cm-thick ash above the S. niagarae zone is equivalent to the youngest layer erupted from the Mono Craters, but that either (a) some radiocarbon ages on organic material in sediments of Walker Lake are biased towards older ages by about 300-400 years, possibly because of inclusion of older detrital carbon or incorporation of older carbon by organisms such as algae in the lake sediments (the reservoir effect), or (b) that Sieh and Bursik's radiocarbon ages of this youngest Mono Craters ash bed are too young. It is also possible

that the 3.4-cm-thick tephra layer at the north end of Walker Lake, correlated by Sieh and Bursik with the youngest eruption from Mono Craters, is either the ca. 950 or 1200-yr-b.p. layer. Some of the disseminated zones of ash above the top of the S. niagarae interval and the 5.5-cm-thick ash (WLC84-8, 3A-14.5-20 cm, depth 2.17 m) might then represent the distal tephra of the youngest Mono Craters eruption. At present, we see no clear choice among these alternatives, but further mapping and more precise petrographic, trace-element, and geochronologic analysis may allow us to resolve this problem.

At the south shore of Mono Lake, tephra from the latest eruption of the Mono Craters is overlain by tephra erupted from the Inyo Craters (Sieh and Bursik, in press). This latter tephra layer is probably the same as the uppermost tephra layer in the Barrett Lake core (fig. 4, tables 1, 2). We estimate the age of this unit to be between 600 and 650 yr b.p., by extrapolation of the sedimentation rate based on radiocarbon ages stratigraphically beneath this layer. This tephra layer is chemically very similar to, and probably equivalent to, surficial pumiceous tephra and tephra in the upper part of soils of mountain meadows south of Mammoth Lakes (sample JANDA-322, table 1). This tephra layer has been equated by Wood (1977) with his tephra layer 1, for which he reports a radiocarbon age of 720 ± 60 yr b.p. This age is on wood and thus may be somewhat older than the associated tephra deposit if the wood is from the inner part of a tree. The ash of Inyo Craters provenance in Walker Lake (WLC84-8-2A, 22-22.5 cm, depth of 2.52 m; table 1) is significantly different in Al, Fe, Ca, and Ti from the Inyo Craters ash in Barrett Lake and from the ash south of Mammoth Lakes (BL-RSA-1, and JANDA-322, respectively; table 1). These data indicate that there were at least two eruptive episodes from the Inyo Craters in latest Holocene time. Barring the existence of reservoir effects, the ages of these eruptions are ca. 600-640 yr b.p. (BL-RSA-1; the 720 yr b.p. eruption dated by Wood, 1977, 1984, may be the same as the ca. 600-640 yr. b.p. eruption), and 1150 yr b.p. (this report). Eruptions from the Inyo Craters both followed shortly after eruptions from the Mono Craters.

Major, minor, and trace-element analyses by XRF and INA of six samples of the youngest tephra layers in cores from Walker Lake (table 4) help to confirm or refine some of the observations made on the basis of EM data. Three samples from Walker Lake core WLC84-8 (2A, 28.5-33 cm, situated at a depth of 2.67 below the water-sediment interface; 3A, 59.5-64 cm, obtained from presumably the same tephra layer but driven deeper into the lake sediments due to a coring malfunction (see above); and 3A, 64-66 cm, situated immediately below the last sample and probably forming part of the same layer) are all chemically indistinguishable and probably are the same tephra layer. Two samples from Walker Lake core WLC84-4 (2, at 3.29 m, and 2, at 3.31 m), are also chemically indistinguishable from the former group of three. All five samples are probably from the same ca. 1200-yr.-b.p. layer, and probably correlate with tephra layer 2 of Wood (1977)(table 4).

Results of XRF and INA analyses also indicate that the lowest tephra layer in Walker Lake core WLC84-8 (8, at a depth of 8.10 m), which we estimate to be about 4650 yr. b.p., is chemically most similar to tephra layer KRL82182(A-3) from Crooked Meadow, estimated to be 3820 yr. b.p. (table 4, fig. 6). These two samples have unusually low scandium values, which distinguish them from other Holocene samples erupted from the Mono Craters. If these two samples are indeed from the same tephra layer, then the

radiocarbon age for this tephra layer obtained at Crooked Meadow is somewhat over 800 years younger than that obtained at Walker Lake. Results of XRF and INA analyses also indicate that the tephra layer at a depth of 8.10 m in WLC84-2 (fig. 5), is most similar to tephra layer KRL82182(A-5) at Crooked Meadow (fig. 6, table 4), estimated to be about 2500 yr. b.p., and may correlate with that layer.

Discussion of ages of upper Holocene tephra layers in Walker Lake and correlative sections at other localities

The interpolated ages of the six young tephra layers in Walker Lake core WLC84-8, based on radiocarbon ages in this core (fig. 6; table 2) are 950, 1150, 1190, 1300, 1800, and 4650 yr b.p. Barring the existence of a reservoir effect, we consider the ca. 1190-yr-b.p. ash bed to be the same as the 1190 \pm 80-yr-b.p. tephra 2, of Wood (1977, 1984). In addition to these tephra layers, there are several zones rich in disseminated glass shards present in Walker Lake core 8 that are chemically quite homogenous (table 2). These zones may represent tephra from minor plinian or phreatic eruptions of the Mono Craters that were disturbed by bioturbation after deposition. Alternatively, these zones may have been produced by reworking of older tephra layers within the Walker Lake basin, but this seems less likely because tephra layers represent a small percentage of Holocene sediments within the Walker Lake basin, and it is difficult to see how reworking within the basin could concentrate the tephra to produce the disseminated zones. Rather, we would expect that reworked tephra be heterogenous, highly diluted with other clastic components of the sediments during reworking, and that redeposited sediments would contain only a low, background level of a few percent or less of glass shards. Some zones of disseminated or deformed tephra below the tephra layer at 2.67-2.71 m in core WLC84-8, on the other hand, may represent portions of tephra layers transposed downward during coring.

Walker Lake core 8 records two late Holocene episodes of volcanic activity of the Mono Craters. Crooked Meadow and Barrett Lake, located east and southwest of Mono Craters (fig. 3), respectively, record similar, broadly contemporaneous episodes of this activity. If the tephra layer sets from these three sites are essentially contemporaneous, then radiometric ages in Barrett Lake appear to be systematically younger than those of Crooked Meadow, and the latter appear to be systematically younger than those of Walker Lake. These data suggest that radiocarbon dates from Walker Lake may include a small reservoir effect, or that radiocarbon dates from Crooked Meadow and Barrett Lake are younger than the actual ages.

Tephra layers in core WLC84-2 at 5.69-8.10 m are chemically similar mostly to those of the younger set (ca. 900-2500 yr b.p.) in WLC84-8, at shallower depths of 2 to 3.5 m, but the layer at 8.14 m in WLC84-2 may be equivalent to older layers of about 7.2 to 7.8 Ka at Crooked Meadow and in Mono Basin, respectively (see below).

Tephra correlations and other age control for the upper part of the section in Walker Lake is unsatisfactory because we are generally unable to distinguish among individual tephra layers erupted from the Mono Craters by EM, and thus unable to correlate associated radiometric age control from other localities to Walker Lake. Consequently, we have not been able to independently verify the accuracy of the radiocarbon ages, particularly with

respect to the possible existence of a reservoir effect in Walker Lake due to the presence of older carbon in the organic and inorganic components of Walker Lake sediments. Furthermore, we were disappointed in not being able to find even one of several widespread, distinctive, well-dated Holocene and latest Pleistocene tephra layers that we might expect to find within this basin. Among these markers are the Mazama (ca. 6.8 Ka), Tsoyowata (ca. 7 Ka), Trego Hot Springs (ca. 23 Ka), Wono (ca. 25 Ka), and Mount St. Helens C (the Marble Bluff ash bed of Davis, ca. 32-37 Ka) ash beds, that have been found in the Carson Sink, about 70 km to the north (Davis, 1978). The Mazama and Tsoyowata ash beds, erupted from Crater Lake, Ore., have been found both to the north of Walker Lake and to the south, in Mono Lake (Sarna-Wojcicki and O. K. Davis, unpublished data, 1988), and thus should have fallen within the Walker Lake basin. The Wono ash bed, also probably erupted from Crater Lake (Davis, 1978), is 5-6 cm thick near Bridgeport, Ca., within the West Walker River drainage basin (Sarna-Wojcicki, unpublished data, 1988), and also should have fallen into the Walker Lake basin. Our inability to find any of these ash beds in Walker Lake suggests that either there were periods of non-deposition in this basin during which any tephra that fell into the basin was subsequently removed by wind, or that sediments containing these layers were not recovered or were so disturbed as to preclude recognition. Whichever the reason, the absence of these critical layers within Walker Lake prevents us from obtaining independent age calibration for latest Pleistocene and Holocene sediments in the lake, and thus diminishes the usefulness of the stratigraphy in this basin as a record of recent climatic change.

Tephra layers at intermediate depths in Walker Lake cores WLC84-4 and 5, near the base of cores WLC84-2 and 3, and in WLC85-2 (ca. 8 to 100 Ka)

Only a few discrete tephra layers were encountered within these cored intervals; most of the samples consisted of disseminated shards that were heterogenous in composition, and thus probably represented reworked detrital tephra, an "ambient" low-level concentration of glass shards derived by erosion of older tephra layers within the drainage basin tributary to Walker Lake, or brought into the lake by wind. Some of these samples are homogenous, however, and the depths and stratigraphic sequences of some homogenous and heterogenous disseminated shard samples are consistent with those of tephra sequences found at other sites within the study area.

Samples of disseminated shards were analyzed by EM only, due to the small sample sizes. Most of the tephra found in Walker Lake sediments within these cored intervals were erupted from the Mono Craters. Discrete tephra layers older than about 4700 radiocarbon yr b.p. have been analyzed from cores WLC84-2, 3, 4, and 5, and WLC85-2 (fig. 5; table 1). Results of these analyses indicate that:

1) A slightly heterogenous population of disseminated Mono Craters-type shards at 16.56 m in core WLC84-4-7B matches well (similarity coefficient, SC, is 0.98, where 1.00 represents a perfect match) with a tephra layer in WLC84-2-3 (8.14 m), with a tephra layer in Mono basin that is stratigraphically close to and beneath the ca. 7 Ka Tsoyowata ash bed (OD-ML-10-445; unpublished data, O. K. Davis and Sarna-Wojcicki, 1988), and with one of the lower tephra layers in Barrett Lake (BL-RSA-10), estimated to be about 7.8 Ka by interpolation of ^{14}C ages (fig. 6).

2) A relatively homogenous sample of disseminated Mono Craters-type shards at 31.81 m in WLC84-4 matches well (SC = 0.99) with Ash Bed 15 in the

Wilson Creek beds of Mono Basin (Lajoie, 1968); the latter is estimated to be 28 Ka by interpolation of ^{14}C ages (K. R. Lajoie, unpublished data, 1988). More heterogenous samples of disseminated shards of similar composition are found within a depth zone from 26.20 to 33.32 m in WLC84-4. A tephra layer of this same composition is present at 20.39 to 20.77 m in WLC84-2, on the east side of Walker Lake, and in pluvial lake beds of Lake Lahontan, in the Carson Sink (Davis, 1978; fig. 9). The Mono Lake magnetic excursion occurs at the level of Ash Bed 15 in the Wilson Creek beds at Mono Basin, and with the same ash bed in Carson Sink (Liddicoat and others, 1982; Lajoie and others, 1983).

3) A homogenous population of disseminated Mono Craters-type shards at 39.81 m in WLC84-4-17 matches well with an ash bed at the South Shore Cliffs, on the south side of Mono Lake. This bed is equivalent to Ash Bed 17 or 19 of the Wilson Creek beds, and thus should be between about 34 and 36 Ka (Lajoie, unpublished data, 1988).

4) A somewhat heterogenous population of disseminated Mono Craters-type shards at 40.08 m in WLC84-5-6 is very similar ($\text{SC} = 0.985$) to a tephra layer at Rush Creek, in the Mono Basin, that overlies charcoal ^{14}C dated at about 32 Ka, and that is chemically equivalent to one of the lower ash beds in the Wilson Creek beds (16, 17 or 19), estimated to be between 33 to 36 Ka on the basis of radiocarbon dates on ostracodes and tufa in Mono Lake (Lajoie, 1968, and K. R. Lajoie, unpublished data, 1988). Zones of disseminated shards very similar to those present near the base of the Wilson Creek beds, and at depths of about 33 to 40 m in Walker Lake cores WLC84-4 and 5, are also found at depths of about 66.5 to 64.5 in these two cores, respectively. Analyses by EM, XRF, and INA, however, favor correlation of tephra at these lower depths to older tephra layers exposed in the Negit Causeway of Mono Basin (see below).

5) - A rather heterogenous population of disseminated shards at 63.06 m in WLC84-5-12, probably erupted from the Inyo Craters or Mammoth Mountain in Long Valley, matches very well ($\text{SC} = 0.98$) with a tephra layer at 9.40 m in WLC85-2 on the southeast side of Walker Lake. The shard chemistry of these samples differs from the Mono Craters types found in the middle intervals of WLC84-4 and 5.

In addition to analyses of disseminated shards, results of EM analysis of discrete tephra layers indicate that the tephra layer at 66.33 m in WLC84-4 matches with that at 64.51 m in WLC84-5, and these match with the ash layer at 21.02 m in WLC84-2 ($\text{SC}'\text{s} = 0.98\text{--}0.99$). Disseminated zones of glass shards also match well between cores WLC84-4 and 5, at depths of about 66.5 (WLC84-4) and 64.5 (WLC84-5). The layer at 66.33 m also matches equally well with tephra layers KRL71082F and KRL71082(II-4) ($\text{SC} 0.986, 0.987$; respectively) of the Negit Causeway, a narrow isthmus between Negit Island and the north shore of Mono Lake exposed due to the temporary lowering of the lake level in historic time, and with 6VI84-1-5.5m ($\text{SC} 0.983$), a tephra layer exposed at the surface north of Walker Lake (Bradbury, written commun., 1986¹).

¹Bradbury, however, suspects that the last layer may be Holocene, based on an inferred stratigraphic relationship between this bed and a tephra layer exposed at a lower elevation nearby.

Results of EM analysis also indicate that tephra samples at 78.77 and 78.91 m from ash beds in WLC84-4-30 and WLC84-5-19, respectively, match well (SC's = 0.983 and 0.975; figs. 5; table 1), and also match with the sample of an ash bed at 38.26 m in WLC85-3, and with the layer KRL71082(II-8) from the Negit Causeway (SC 0.989)(fig. 9).

Results of more recent XRF and INA analyses confirm some of the correlations inferred on the basis of EM analysis (items 6 and 7), and provide some additional correlations as well (table 5). The tephra layer at 64.51 m in core WLC84-5 correlates well with the late Pleistocene tephra layer exposed in the Negit Causeway of Mono Lake, KRL71082(II-4), on the basis of XRF, INA, as well as EM analyses (SC for 27 elements based on all three analytical methods is 0.96)(table 5; fig. 9). The tephra layer at 78.91 m in the same core, WLC84-5-19, correlates marginally by all three methods with the tephra layer at 78.77 m in WLC84-4-30 (SC = 0.93 for 27 elements determined by EM, XRF, and INA). The latter tephra layer correlates well with the layer at 38.26 m in WLC84-3-7 (SC = 0.96), and both WLC84-4-30 and WLC84-3-7 correlate well with KRL71082(II-8), a tephra layer from the late Pleistocene section at the Negit Causeway (SC's of 0.96 and 0.97, respectively, for the suite of 27 elements analyzed by EM, XRF, and INA). The last tephra layer stratigraphically underlies tephra layer KRL71082(II-4) by about 2.5 m; the latter tephra layer in turn, correlates with the tephra layer at 64.51 m in WLC84-5 (table 5; fig. 9). These correlations are thus consistent with the observed stratigraphic sequence at both Walker Lake and the Negit Causeway at Mono Lake. Results of XRF analysis also indicate that the tephra layer at 13.65 m in core WLC85-2, at the south shore of Walker Lake, correlates well with the tephra layer at 78.91 m in WLC84-5 (SC = 0.97), but only marginally with other samples that we have identified as correlatives of the latter layer on the basis of both XRF and INA analyses (WLC84-4-30, 78.77 m; WLC84-3-7, 38.26 m; and KRL71082(II-8); SC's of 0.92 to 0.93).

Two other tephra layers present in the Negit Causeway section (KRL70182(II-3) and KRL70182(II-5); table 5), are interbedded with the two tephra layers (KRL71082(II-4) and KRL71082(II-8)) that we correlate on the basis of EM, XRF, and INA analysis with the two tephra layers at intermediate levels in WLC84-4 and 5, at depths of about 65 and 79 m, respectively (fig. 9). The stratigraphic sequence of these layers at the Negit Causeway, from bottom to top, is II-8, II-5, II-4, and II-3 (fig. 9). Tephra layers II-5 and II-3 are chemically similar to tephra erupted from Mammoth Mountain, in the Long Valley caldera (Bailey, 1976; R. Bailey, written commun., 1988). They are particularly similar to a rhyolite flow, KDP-73-140 (analysis shown in table 5; compare with II-5 and II-3). Because the whole-rock composition of the rhyolite, which contains biotite and feldspars, is compared with glass analyses of the tephra layers, some large differences are apparent in the alkali-earth and transition elements that tend to be concentrated in these phenocrysts. The similarity in the rare-earths and some of the heavier metals (Hf, Ta, Th, and U), however, is striking, and we conclude that these two tephra layers were erupted from the same source, the Mammoth Mountain area. According to Bailey (1976), Mammoth Mountain was active during a period about 50 to 150 Ka yr. b.p.

Discussion of correlation of tephra layers at intermediate depths
in WLC84-4 and 5, near the base of WLC84-2 and 3, and in WLC85-2

The correlations documented above and in table 1, and shown in figure 9, suggest that the sediments at a depth of about 16.5 m in WLC84-4 are about 7 to 8 Ka; at 32 to 40 m in WLC84-4 and 5, about 28 to 36 Ka; at 64 to 79 m, of rather indeterminate age but probably between about 50 and 150 Ka based on their correlation to the Negit Causeway in Mono Basin and, in turn, of associated tephra layers at the latter locality to Mammoth Mountain in Long Valley.

Correlations made on the basis of all three analytical methods, EM, XRF, and INA, for samples at intermediate depths in WLC-4 and 5 support those made on the basis of EM data. These correlations indicate that the tephra layer at 13.65 m in core WLC85-2 near the south shore of Walker Lake correlates with the layer at 38.26 m in WLC84-3, in the east-central part of the lake, and with the layers at 78.77 and 78.91 m in WLC85-4 and 5, respectively, in the west-central part of the lake (table 5; fig. 9). This tephra layer correlates, in turn, with the tephra layer in the Negit Causeway (KRL71082(II-8)). Because tephra layers at about 65 and 79 m in WLC84-4 and 5 correlate with late Pleistocene tephra layers of the Negit Causeway, and because the latter are interbedded with tephra layers erupted from Mammoth Mountain, erupted about 50 to 150 Ka, these data provide some broad age constraints on the tephra layers at intermediate depths in the Walker Lake cores. This age constraint is compatible with Lajoie's (1968) estimate of greater than 40 Ka for these layers.

The above correlations indicate that sediments thicken from the west-central part of the Walker Lake basin, from about 21 m at WLC84-2 on the east side of the lake, to about 65 m at WLC84-4 and 5, on the west side; and from about 14 m in WLC85-2 at the south shore of the lake, to about 38 m in WLC84-3 at the east side, and to about 79 m in WLC84-4 and 5, on the west side of the lake (fig. 5).

Lowermost tephra layers in Walker Lake cores
WLC84-4 and 5 (ca. 300-370 Ka)

The oldest tephra layers and zones of disseminated glass shards in WLC84-4 and 5 are at depths of about 142 to 146 m (figs. 5 and 9; table 1). These tephra layers were probably erupted from the Cascade Range in Oregon, as indicated by their chemical similarity to tephra erupted from that source.

The samples taken from a 2-cm interval at 141.78-141.80 m in WLC84-5 (table 1) match well with an ash bed in Summer Lake, Ore. (sample DR30W of Bed JJ of Davis, 1985), as well as with a tephra layer exposed on Paoha Island, in Mono Lake (PAOH 1; SC 0.96 for 8 elements¹; table 1, fig. 9). We estimated the age of this tephra layer by correlating overlying and underlying ash beds

¹/Because glasses in the more basic tephra layers contain higher concentrations of MgO and TiO₂ than silicic tephra, eight elements rather than six can be used in the comparison. Basic glasses, however, tend to be more heterogeneous than silicic glasses, and consequently lower values of the similarity coefficient are frequently obtained.

at Summer Lake to tephra layers at Tululake, Ca.. Using an age-vs.-depth sedimentation-rate curve derived on the basis of age control developed for the latter site, we estimate the ages of the ash beds correlated between Summer Lake and Tululake. These estimated ages are then used to interpolate the age, about 300 Ka, of ash bed JJ at Summer Lake (Sarna-Wojcicki, Rieck, Meyer, and Adam, unpublished data).

The tephra layer at 143.75 m in WLC84-4 matches well with an upper-Pleistocene tephra layer at Tululake, Calif. (T2023, at 53.07 m in Tululake core 5). We estimate this tephra layer to be about 360-370 Ka, as interpolated from age data at Tululake (Sarna-Wojcicki, Rieck, Meyer, and Adam (unpublished data, 1988) (fig. 9, table 1). This tephra layer also correlates to ash bed KK at Summer Lake (Devis, 1985), which underlies the abovementioned ash bed JJ.

Correlations and stratigraphic relationships of the older tephra layers in Walker Lake cores WLC84-4 and -5, and at other sites (fig. 9), indicate that stratigraphic sequences at all correlated sites are consistent with the correlations proposed here. If the correlations were fortuitous or random, we would expect about half of the correlation tie lines (fig. 9) to cross.

Most of the tephra layers in the lower parts of WLC84-4 and -5 were too thin to provide enough sample for XRF and INA analyses. The sample at 141.78 m in WLC84-5 was analyzed by XRF despite its small size, and matches best with the tephra layer from Paoha Island, in Mono Lake (PAOH-1; table 6), as inferred above on the basis of EM data, although the intensities for some of the minor and trace elements were too low to provide an adequate basis for comparison. The tephra layer on Paoha Island (PAOH-1) is part of a sequence of three tephra layers (from base to top, PAOH-2, PAOH-1, and PAOH-3; fig. 9, table 6; fig. 9), two of which (PAOH-2 and PAOH-3) correlate with tephra layers in lacustrine deposits of Lake Crowley in Long Valley Caldera (M7811 and KRL10779, respectively; table 6). A magnetic reversal is associated with the uppermost tephra layer at Paoha Island (PAOH-3), and with the correlative layer at Benton Crossing (KRL10779) (Liddicoat and others, 1980). Our estimate of the age of this layer based on the age control from Tululake is about 280 Ka, close to the 290 Ka estimated age of the Biwa 2 magnetic reversal (Yaskawa and others, 1973), and thus may be this reversal.

Summary and Discussion

Data on tephra correlations presented here is tentative for the upper part of Walker Lake sediments in cores WLC84-2 through 5, 8, and WLC76-G (0 to about 12 m), because most of the tephra layers in this interval were erupted from the Mono Craters, and tephra layers from this source are chemically very similar and difficult to distinguish on the basis of probe analysis. Consequently, associated radiometric and other numerical age data obtained outside of the Walker Lake basin could not be correlated to the basin with a high degree of confidence. An alternative way of providing independent checks on radiocarbon ages in Walker Lake was foiled by our failure to find and identify any of the more distinctive, widespread, well-dated latest Quaternary tephra layers such as the Mazama and Wono ash beds. This failure may be due to poor core recovery, disturbance during drilling, or to lack of preservation of these layers during lowstands of the lake. Consequently, we are unable to independently determine the presence or magnitude of a possible reservoir effect in the radiocarbon dates determined on Walker Lake sediments.

Using several lines of evidence and assuming that no reservoir effect is present in the radiocarbon dates, we correlate a tephra layer in several cores of Walker Lake with the widespread ca. 1200-yr-b.p. Mono Craters tephra layer (tephra 2 of Wood, 1977).

The tephra layers and disseminated zones of shards at depths of about 32 to 40 m in WLC84-4 and 5, and at about 20 to 21 m in WLC84-2, appear to correlate with the middle to lower part of the Wilson Creek beds of Lajoie (1968), and are thus probably about 28-36 Ka. The Wilson Creek beds on the north side of Mono Basin contain a suite of 19 tephra layers, 18 of which were erupted from the Mono Craters, and one, basaltic in composition, erupted from Black Point, a volcano on the north shore of Mono Lake (Lajoie, 1968). These tephra layers range in age from about 36 Ka to 12 Ka b.p., (Lajoie, 1968; Lajoie, unpublished data) and are interbedded with lacustrine sediments that represent continuous deposition in Mono Lake during this time. At least one of these layers, Ash Bed 15, has been found as far north as the Carson Sink (Liddicoat and others, 1982), about 70 km north of Walker Lake. It is puzzling why only a couple of these layers have been found in the deeper cores, WLC84-4 and -5, on the west side of the lake. Poor core recovery or sediment disturbance may be the cause, although some of the tephra layers in the Wilson Creek beds are fallout from small eruptions that deposited tephra locally, and did not reach Walker Lake.

In figure 10, we plot the available radiocarbon ages (Yang, 1988) and correlated tephrochronologic ages against depth for the upper 40 m of sediments in cores from the west-central part of Walker Lake (WLC-84-4, 5, 6, and 8), the present depositional center of the lake. We also plot on this figure the position of two dessication events determined from ^{18}O isotope analysis of ostracode carapaces, and two porosity changes (Benson, 1988). We have drawn a sedimentation-rate curve that attempts to provide a best fit to this data. The curve is fairly well constrained by the available data except for the intervals from 15 to 20 m and 35 to 40 m, where the age data are scattered. Abrupt changes in sedimentation rate can be made to fit the two dessication events and one porosity change (33-35 m), and still conform to most of the age-depth data points. The other porosity change, at 15 m, however, does not correspond to any change in the sedimentation-rate curve as we have drawn it. An alternative curve segment (dashed curve segment in fig. 10) corresponds with the porosity change, but is further from age control points. Nevertheless, the overall fit of the age vs depth data, and positions of identified dessication events and porosity transitions is good, and this curve can be regarded as an approximate record of the history of sedimentation in Walker Lake basin, a record that reflects the composite effects of both climate and drainage history for this basin during the last 40 Ka.

The shallow lake levels and frequent dessication events inferred for the interval of intermediate porosity at depths of 35 to 15 m in the deep Walker Lake cores (WLC84-4 and 5; Benson, 1988), corresponding to an age range of about 32 to 9 Ka before present (roughly, the last glacial stage, or oxygen-isotope stage 2 of Shackleton and Opdyke, 1976), are anomalous when compared to such late Pleistocene Great Basin lakes as Russell (Mono), Bonneville, and other parts of Lake Lahontan. Lake levels in these lakes were high and deposition was presumably rapid and continuous during the last glacial stage (Benson, 1988; Lajoie, 1968, and unpublished data, 1988). Walker Lake, however, seems to have had a variable depositional history during this time,

one that can perhaps be best explained by a combination of drainage and climate changes, rather than by climate changes alone. The Walker River has changed course at Adrian Pass one or more times in the past, flowing either into Walker Lake or the Carson Sink (King, 1978; Davis, 1982), and this may account for some of the variability in the sedimentation rate in Walker Lake during this time interval, as compared to other large lakes in the Great Basin. Benson (1988), however, has shown that tufa and shorelines in the Walker Lake subbasin were high (1330 m) and contiguous with Lake Lahontan during the period 14 to 12.5 Ka ago. Consequently, the discordance in the sediment record between Walker Lake and other sites for this smaller time span may result from poor core recovery in Walker Lake.

An alternative explanation for the inferred slow-down of sedimentation in the depositional center of Walker Lake at about 12 Ka ago, as suggested by the solid curve in figure 11, is that a rapid rise in lake level at about this time would temporarily shift the locus of sedimentation toward the north by drowning the lower reaches of Walker River. Rapid sediment deposition at the site would not resume until Walker Lake sediments had prograded back out to the depositional center sometime after lake level had stabilized or begun to fall.

The lowest layer at 21.02 m in WLC84-2 may correlate with the 64 to 67-m levels in WLC84-4 and 5, and with a tephra layer (KRL71082(II-4)) in the upper part of a sequence of late Pleistocene tephra layers at Negit Causeway in Mono Lake, which are estimated to be greater than about 40 Ka, and between 50 and 150 Ka in age, based on correlation of two other tephra layers in the latter sequence to Mammoth Mountain in Long Valley caldera. Such a correlation, however, would require that a hiatus be present in WLC84-2, just above the lowest layer, because the tephra layer close above, sampled at 20.39 and 20.77 m, matches well with the younger Wilson Creek ash bed 15, dated at 28 Ka (fig. 5). Tephra samples in Walker Lake sediments at 13.65 m in WLC85-2, at 38.26 m in WLC84-3, at 78.77 m in WLC84-4, and at 78.99 m in WLC84-5 comprise a single, correlatable layer in Walker Lake, and correlate with a tephra layer (KRL71082(II-8)) in the lower part of the Negit Causeway section, estimated to be between about 50 to 150 Ka (as above).

The lowest tephra layers recovered from Walker Lake sediments, at about 142 to 145 m in WLC84-4 and 5, correlate with upper middle Pleistocene layers at Summer Lake, Ore., and at Tulelake, Calif. The tephra layer at 141.78 m in WLC84-5 correlates with bed JJ at Summer Lake (Davis, 1985), and is estimated to be about 300 Ka. The tephra layer at about 145 m in WLC84-4 correlates chemically with a tephra layer at Tulelake (T2023), estimated to be 360-370 Ka on the basis of age control determined at the latter site, and with a tephra layer at Summer Lake, Ore. (ash bed KK of Davis, 1985). Given the uncertainties in these age estimates and probable existence of compounding errors, the error in the estimate of the age of the tephra layer at 141.78 m may be as much as ± 50 Ka, and that of the layer at about 145 m, $+30$ to -50 Ka.

Agreement in stratigraphic sequence among correlated tephra layers and bracketing tephra layers at several sites support most correlations of the ash layers at intermediate and lowest depths in the Walker Lake cores (fig. 9), and these correlations appear to be more definitive than those of Mono Craters tephra layers in the uppermost 12 meters of Walker Lake sediments. In this context, however, we should point out that the resolution of the chemical

"fingerprinting" technique for suites of very homogenous tephra layers such as those erupted from Mono Craters may be only ± 1000 yrs, when we use the EM method, and may not be much better for the XRF method. Such resolution is very good compared to other numerical geochronologic methods at 300 Ka, still respectable at 30 Ka, but nearly fatal at 2 Ka. The compositional resolution required to distinguish between chemical types in INA analysis is much better than it is in EM or XRF analysis, but it is difficult to use this technique on small samples such as those obtained from cores, and the method is expensive and slow; it may eventually provide better age control.

At 85 to 119 m in WLC84-5 and at 145.24 m in WLC84-4 there are some disseminated glass shards of heterogenous composition that are chemically similar to older tephra layers erupted from the Long Valley-Glass Mountain volcanic source areas. These shards are probably reworked from some of the voluminous, older tephra layers, such as the Bishop Tuff (0.74 Ma), the ash beds of Glass Mountain (ca. 0.9 and 1.0 Ma), and older tephra of the Tuff of Taylor Canyon (ca. 2.0 to 3.3 Ma) (Sarna-Wojcicki and others, 1984; Metz and Mahood, 1985), and are a "background-level" contaminant derived by erosion within the drainage basin of Walker Lake, or were brought in by wind.

Because none of the widespread, voluminous, middle Pleistocene (400-700 Ka) tephra layers found throughout the Great Basin and other parts of the conterminous western United States are present as discrete beds in cored sediments of Walker Lake, a maximum possible age of about 400 Ka for the oldest sediments recovered appears to be reasonable. For instance, the Rockland ash bed, dated at about 400 Ka by fission-track and K-Ar analyses (Meyer and others, 1980; Sarna-Wojcicki and others, 1985; Meyer and others, unpublished data, 1988) has not been found in WLC84-4 or 5, even though Walker Lake probably lies within the fallout area of this ash, and the Walker Lake basin probably represented a favorable depositional site at that time. This ash is present about 75 km to the southwest, near Bridgeport, Calif., in the drainage of the West Walker River that is tributary to Walker Lake (Sarna-Wojcicki and others, 1985), and is about the same distance away from the source of the eruption (the Lassen peak area of northeastern California) as is Walker Lake, and at a similar azimuth. Similarly, we have not identified the Dibekulewe (ca. 0.4 to 0.6 Ma), Lava Creek B (0.62 Ma), or Bishop (0.74 Ma) ash beds in these cores, even though Walker Lake was probably within the fallout area of these ash falls. This is most emphatically the case for the Lava Creek B ash bed, which has been identified east, north, west, and south of Walker Lake (Davis, 1978; Izett and Wilcox, 1982; Sarna-Wojcicki et al., 1984). The Lava Creek ash bed is about 3 m thick at Lake Tecopa, in southeastern California, about 340 km southeast of Walker Lake, and lies at a similar azimuth as Walker Lake from the eruptive source in the Yellowstone National Park area, although considerably farther away than Walker Lake. The Lava Creek B ash bed was deposited during a pluvial period in the Great Basin (Sarna-Wojcicki and others, 1984), and should be present at favorable sites such as Walker Lake.

In figure 11, we present a tentative age-depth curve that summarizes the available age control for late Quaternary sediments of Walker Lake, and some of the major sedimentological changes observed in the sediments (Benson, 1988). Because of problems in core recovery, depth registration, drilling-induced sediment deformation, the consequent inability to derive a magneto-stratigraphic record, and absence of many diagnostic, well-dated tephra

layers, the chronology for sediments in Walker Lake is tenuous.

Abrupt changes in porosity and variations in the inferred sedimentation rate within Walker Lake suggest that sedimentation in the basin was not continuous during late Quaternary time. The inferred change in sedimentation rate at 100-105 m in WLC84-4 and 5, which we have drawn to coincide with a change in sediment porosity (Benson, 1988), is particularly striking. Low porosity of sediments below this level suggest that shallow or dry conditions frequently existed in Walker Lake basin during deposition of sediments between the ca. 150 to 105 m depth (Benson, 1988), or that the sediments were preconsolidated by subaerial exposure. A slow inferred sedimentation rate during this period (fig. 11) supports this observation, although this could also be achieved by a smaller sediment contribution to Walker Lake than that which entered later. The high porosity interval above the porosity change, between about 105 and 35 m, by contrast, suggests that lake levels were moderate to high (Benson, 1988), and the sedimentation curve suggests that deposition was rapid (fig. 11). There are at least three possible explanations for the porosity/sedimentation rate change at the 100-105 m level:

- 1) The denser sediments below about 105 m in Walker Lake were consolidated during a dry/hot¹ period of long subaerial exposure; the less dense sediments were deposited during a wet/cool period, and the porosity/sedimentation rate change between them represents a period of very slow deposition or a hiatus.

- 2) Because the Walker River has changed course at Adrian Pass one or more times in the past, the Walker River may have discharged into the Carson Sink during the time of deposition of the lowermost sediments (about 105 to 150 m), and consequently sediment influx and the lake level were low; Walker River then switched into the Walker Lake basin at the time represented by the change in porosity/sedimentation rate.

If the first explanation is correct, existing age constraints and climatic aspect would argue that the hiatus corresponding to the change in porosity occurred during the dry/hot oxygen-isotope stage 5 (ca. 85 - 136 Ka; Shackleton and Opdyke, 1976)(fig. 11). The subsequent period of rapid sedimentation and high porosity, consequently, would correspond mainly to oxygen-isotope stage 4, and possibly to stage 3 and part of stage 2 as well. Other scenarios are, of course, possible. However, oxygen-isotope stage 5 probably corresponds to the longest and most intensive recent hot/dry period in the Western U.S.. Sediments deposited prior to this period would be dessicated and compacted, and there would be minimal stream discharge and sediment deposition, and perhaps even aeolian erosion, in lake basins of the Great Basin during this time. If the second explanation is correct, however, then the changes in porosity and sedimentation rate need not all coincide with climatic changes, although the latter would presumably also affect overall sedimentation rates as well.

- 3) A third explanation for the change in porosity at 100-105 m in the

¹Dry and/or hot. The low lake levels are an effect of decreased "effective moisture", and could be an effect of either hot and dry or cool and dry conditions (Benson, written commun., 1988).

deeper Walker Lake cores is a consequence of the geometry of the Walker Lake basin. This basin is an elongate, asymmetrical trough (figs. 1 and 3) bounded by linear ranges on both sides. Its primary sediment source is from the Walker River drainage, which enters the basin from the north. Filling of the basin has thus proceeded from north to south, displacing the lake southward, except for periods when the Walker River drainage may have shifted to the Carson Sink at Adrian Pass. At such times, the smaller local basins would become the predominant sources of sediment, the sediment sources would be distributed more symmetrically within the basin, and the rate of sediment input would be slower. Thus, when the Walker River drainage flowed into the Walker Lake basin, the depositional center of the basin probably shifted southward (and upward) through time as lake sediments prograded from the north towards the south. The present depositional center of the basin (the deepest part of the lake) should thus lie south and somewhat higher than a series of older depositional centers now buried by the prograding Walker River delta and its prodeltaic sediments. A deep core drilled at the present depositional center should thus encounter older sediments that lay on a north-facing paleoslope situated to the south and slightly higher in elevation than their coeval depositional center. In a basin which has experienced shifting lake levels through time, such geometry almost requires that gaps in the stratigraphic record be encountered at a coring site within the present depositional center. Sediments below such gaps should be more consolidated by subaerial exposure and weathering than younger lake sediments above. To give a further illustration of this idea: if the level of Walker Lake should rise and lake sediments prograde further south to a depositional center near the vicinity of core WLC85-2, a core at the new depositional center would encounter a condensed section of older, preconsolidated sediments such as those we encountered in WLC85-2, beneath the new lake sediments that are deposited at this center, and a hiatus would be present between the old and new sediments. The condensed section within the older sediments is a consequence of both subaerial dehydration and consolidation, as well as of slower sedimentation rates that existed on the south slope of the basin, away from the main clastic sediment source to the north. This last explanation for the change in sediment characteristics at about 100-105 m in the two deep Walker Lake cores is quite likely, and is also compatible with either of the first two hypotheses.

Further work is needed to refine the age control in Quaternary sediments of Walker Lake, and to test the hypotheses proposed here. The current state of knowledge regarding the stratigraphy, chronology, and drainage history of late Quaternary sediments in Walker Lake is incomplete. Available age and stratigraphic data suggest that the history of sedimentation in Walker Lake may be different than that of other pluvial lakes in the Great Basin because of changes in the drainage basin tributary to Walker Lake. It thus appears that Walker Lake cannot be used by itself as a reference section for late Quaternary paleoclimatic change in the western Great Basin, but must be complemented by studies at other sites in this region. Progress in unraveling the paleoclimatic history of Walker Lake would benefit from a relatively undisturbed and continuous core in sediments of this lake somewhat north of the present depositional center, to obtain better independent age control from tephrochronology and megnetostratigraphy. Concurrent work on other sections such as that in Crooked Meadow, and in the Wilson Creek beds and on Paoha Island in Mono Lake, and additional uranium-series age analyses currently under way, may provide more precise age control than is presently available.

Acknowledgements

We thank J. L. Slate for performing energy-dispersive spectrometric analyses of tephra samples, and J. Budahn, D. Knight, and D. McKown for performing instrumental neutron activation analyses on tephra samples. We thank R. H. Fehr and Mike Hamer for separating volcanic glass from tephra samples and preparing separates for analysis. We are also grateful to William Thordarson for making smear slides of the deep cores in Walker Lake, and examining them for the presence of disseminated volcanic glass shards, as well as for his assistance to us during sampling of the cores. We are grateful to J. P. Bradbury and R. M. Forester for helping to improve the manuscript and for useful discussions on the subject of this report. We also appreciate useful discussions with H. J. Rieck, Larry Benson, R. A. Bailey, and J. O. Davis, and the information they provided to this report.

References

- Benson, Larry, 1988, Preliminary paleolimnologic data for the Walker Lake subbasin, California and Nevada. U.S. Geological Survey, Water-Resources Investigations Report 87-4258, 50 p.
- Bradbury, J. P., 1987, Late Holocene diatom paleolimnology of Walker Lake, Nevada. *Archiv fur Hydrobiologie*, Suppl.-Bd. 79, 1, 27 p.
- Borchardt, G. A., Aruscavage, P. J., and Millard, H. T. Jr., 1972. Correlation of the Bishop ash, a Pleistocene marker bed, using instrumental neutron activation analysis. *Journal of Sedimentary Petrology*, v. 42, p. 301-306.
- Davis, J. O., 1978. Quaternary tephrochronology of the Lake Lahontan area, Nevada and California. University of Nevada, Reno, Nevada Archeological Survey, Research Paper 7.
- Davis, J. O., 1982. Bits and pieces: the last 35,000 years in the Lake Lahontan area, in Madsen, D. B., and O'Connell, J. F., eds., *Man and environment in the Great Basin*. Society of American Archeology Papers, no. 2, p. 53-75.
- Davis, J. O., 1985. Correlation of late Quaternary tephra layers in a long pluvial sequence near Summer Lake, Oregon. *Quaternary Research*, v. 23, p. 38-53.
- Izett, G. A., and Wilcox, R. E., 1982. Map showing localities and inferred distributions of the Huckleberry Ridge, Mesa Falls, and Lava Creek ash beds (Pearlette family ash beds) of Pliocene and Pleistocene age in the western United States and Canada. U.S. Geological Survey Miscellaneous Investigations Series Map I-1325.
- King, G. Q., 1978, the late Quaternary history of Adrian Valley, Lyon County, Nevada. Unpublished M.S. Thesis, Department of Geography, University of Utah.
- Lajoie, K. R., 1968. Quaternary stratigraphy and geologic history of Mono basin, eastern California. University of California, Berkeley, PhD dissertation.
- Lajoie, K. R., Sarna-Wojcicki, A. M., Robinson, S. W., and Liddicoat, J. C., 1983, Late Pleistocene stratigraphic correlations and lacustrine histories in the western Great Basin, Geological Society of America, Abstracts with Programs, Rocky Mountain-Cordilleran Section, v. 15, no. 5, p. 300.
- Liddicoat, J. C., Lajoie, K. R., Bailey, R. A., Sarna-Wojcicki, A. M., Russell, P. C., and Woodward, M. J., 1980, Reversal of the paleomagnetic field in Brunhes-age lacustrine sediments in Long Valley and Mono Basin, California. American Geophysical Union, Abstracts with Program, EOS, v. 61, no 17, p. 215.
- Metz, Jenny, and Mahood, Gail, 1985. Eruptive history of Glass Mountain, Long Valley, California: precursors to a large explosive eruption. *Proceedings*

- of Workshop XIX, Active Tectonic and Magmatic Processes Beneath Long Valley, Eastern California. U.S. Geological Survey Volcano Hazards Program, U.S. Geological Survey Open-File Report 84-939, v. 1, p. 41-75.
- Meyer, C. E., Woodward, M. J., Sarna-Wojcicki, A. M., and Naeser, C. W., 1980, Zircon fission-track age of 0.45 million years on ash in the type section of the Merced Formation, west-central California. U.S. Geological Survey Open-File Report 80-1071, 9 p.
- Sarna-Wojcicki, A. M., 1976, Correlation of late Cenozoic tuffs in the central Coast Ranges of California by means of trace- and minor-element chemistry. U.S. Geological Survey Professional Paper 972.
- Sarna-Wojcicki, A. M., Bowman, H. R., Russell, P.C., 1979. Chemical correlation of some late Cenozoic tuffs of northern and central California by neutron activation analysis of glass and comparison with X-ray fluorescence analysis. U.S. Geological Survey Professional Paper 1147.
- Sarna-Wojcicki, A. M., Bowman, H. R., Meyer, C. E., Russell, P. C., Woodward, M. J., McCoy, Gail, Rowe, J. J., Jr., Baedeker, P. A., Asaro, Frank, and Michael, Helen, 1984. Chemical analyses, correlations, and ages of upper Pliocene and Pleistocene ash layers of east-central and southern California. U.S. Geological Survey Professional paper 1293.
- Sarna-Wojcicki, A. M., Meyer, C. E., Bowman, H. R., Hall, N. T., Russell, P. C., Woodward, M. J., and Slate, J. L., 1985. Correlation of the Rockland ash bed, a 400,000-year-old stratigraphic marker in northern California and western Nevada, and implications for middle Pleistocene paleogeography of central California. Quaternary Research, v. 23, p. 236-257.
- Shackleton, N. J., and Opdyke, N. D., 1976. Oxygen-isotope and paleomagnetic stratigraphy of Pacific core V28-238, late Pliocene to latest Pleistocene. Geological Society of America Memoir 145, p. 449-464.
- Sieh, Kerry, and Bursik, Marcus, in press. Most recent eruption of the Mono Craters, eastern California. Journal of Geophysical Research.
- Stuiver, Minze, and Becker, Bernd, 1986, High precision decadal correction of the radiocarbon time scale, AD 1950-2500 BC. Radiocarbon, v. 28, no. 2B, p. 963-910.
- Stuiver, Minze, and Reimer, P. J., 1986, A complete program for radiocarbon age calibration, 1986, Radiocarbon, v. 28, no. 2B, p. 1022-1030.
- Wood, S. H., 1977. Distribution, correlation, and radiocarbon dating of late Holocene tephra, Mono and Inyo Craters, eastern California. Geological Society of America Bulletin, v. 88, p. 89-95.
- Yang, I. C., 1988, U.S. Geological Survey, Denver, Colorado, Radiocarbon Dates V. Radiocarbon, v. 30, no. 1, p. 41-50.
- Yaskawa, K., Nakajima, T., Kawai, N., Torii, M., Natsuhara, N., and Horie, S., 1973, Paleomagnetism of a core from Lake Biwa (1). Journal of Geomagnetism and Geoelectricity, v. 25, p. 447-474.

Figures

Figure 1. Sites in the western conterminous United States where age control for sediments of Walker Lake is obtained by means of tephra correlation. Map base is from U.S. Geological Survey shaded relief map, scale 1:7,500,000.

Figure 2. Location of sediment cores in Walker Lake (from Benson, 1988).

Figure 3. Location of cores and exposures south of Walker Lake where tephra layers are found that correlate or may correlate with those in Walker Lake.

Figure 4. Graphic logs of Walker Lake cores WLC84-8, WLC75-E, and WLC76-G, the Crooked Meadow section, and the core in Barrett Lake. Solid lines and boxes with "v" pattern indicate positions of tephra layers. Dashed lines within cores indicate positions of zones of disseminated glass shards. Dashed tie lines between sites indicate probable correlations. Black bars indicate positions of radiocarbon ages. ^{14}C analyses on disseminated organic material (O), carbonate (C), peat (P), and wood (W). Radiocarbon ages for WLC84-8 from Benson (1988) and Yang (1988); for WLC75-E, from L. Benson, as cited in Davis (1978); for Crooked Meadow, from K. R. Lajoie and S. W. Robinson, unpublished data, (1986); and from Barrett Lake, from R. S. Anderson (written communication, 1986).

Figure 5. Graphic logs of Walker Lake cores WLC84-2 through 5. Solid lines within cores indicate positions of tephra layers analyzed to date. Ticks on either side of cores indicate supplementary samples collected in February, 1986, to test for presence of additional disseminated zones of glass shards or thin tephra layers not detected during initial sampling. Those samples from the latter group that contained glass and were analyzed are marked with a "G". Dashed lines between cores indicate correlations.

Figure 6. Sedimentation-rate curves (solid sloping lines) for Walker Lake core WLC84-8, the Crooked Meadow section, and the Barrett Lake core. Deposition of ash beds is assumed to be instantaneous. Boxes represent radiocarbon ages; width of boxes represents analytical error in age analysis; height of boxes represents interval of core or section sampled for radiocarbon analysis. Dashed lines connect youngest radiocarbon age at each site with assumed zero age of top of core or section. Dashed line below the youngest radiocarbon age for the Barrett Lake core represents adjustment of sedimentation-rate curve to make thickest of the upper set of Mono Craters tephra layers (BL-RSA-4) equivalent in age to Wood's (1977) tephra layer 2.

Figure 7. Sedimentation-rate curves (solid sloping lines) for Walker Lake cores WLC75-B, -D, -E, WLC76-G, and WLC84-8. Boxes represent radiocarbon ages, as in figure 6. Circles represent positions (bases) of tephra layers. Broken circles represent zones of disseminated glass shards. Dashed lines represent sedimentation-rate curves plotted using radiocarbon ages corrected for past atmospheric ^{14}C variation. Ages shown on the figure are based on uncorrected radiocarbon ages. Ages in parentheses are based on corrected radiocarbon ages. Triangles represent the top of the Stephanodiscus niagarae interval (Bradbury, 1987; see text). IC - tephra layer erupted from Inyo Craters; MC - tephra layers erupted from Mono Craters.

Figure 8. Ages of late Holocene tephra layers (wide horizontal lines) and zones of disseminated glass shards (short horizontal lines) in Walker Lake core WLC84-8, the Crooked Meadow section, and in the Barrett Lake core. All tephra layers and zones were erupted from the Mono Craters except for those marked IC, which are from the Inyo Craters. Zones of uncertainty in age/stratigraphic position for deformed beds are represented by dashed vertical lines and queries.

Figure 9. Correlation chart for tephra layers in Walker Lake cores, and tephra layers found at some sites in the western conterminous United States and northwestern Pacific Ocean. See figures 2 and 3 for locations of sites. Solid tie lines indicate tephra correlations based on electron-microprobe (EM) analysis; dashed tie lines with queries indicate probable correlations based on EM analysis. Additional tie lines indicate those correlations that are supported by X-ray fluorescence (XRF) and instrumental neutron activation (INA) analyses. Data for Tullake core from Sarna-Wojcicki, Rieck, Meyer, and Adam, unpublished data, 1986.

Figure 10. Sedimentation-rate curve drawn on the basis of available radiocarbon (Yang, 1988) and correlated tephra ages (this report), and sedimentological changes (Benson, 1988) within the cores near the depositional center of Walker Lake (WLC84-4, 5, 6, and 8), for the upper 40 m of sediments. The curve (solid line) is an attempt to provide a best fit to all available chronologic and stratigraphic data. Major sedimentological changes (porosity and dessication) can be accommodated by most of the constraining age data except for the porosity change at 15 m. An alternative segment of the curve (short dashes) would accommodate this porosity change, but would be further away from more of the age control points. Age control points are shown as circles. Numbers next to age control points correspond to the core numbers (for example, 4 to core WLC84-4, etc.). O - radiocarbon age on organic material; I - radiocarbon age on inorganic material; T - correlated tephra age. Horizontal and vertical bars represent age and stratigraphic error, respectively. (MIN.) - minimum age.

Figure 11. Age vs. depth (sedimentation-rate) curve for upper Quaternary sediments in Walker Lake. Shaded area represents the general range of possible age vs. depth relationships for sediments in cores WLC84-4 and 5, as constrained by available age control. ^{14}C - radiocarbon date; U-series - uranium-thorium series date (Benson, 1988). The solid and dashed sloping line represents a sedimentation-rate curve, assuming a hiatus or very slow-sedimentation rate during oxygen-isotope stage 5 (ca. 85-136 Ka), and a control of sedimentation rate that corresponds generally to glacial-interglacial or oxygen-isotope stages (Shackleton and Opdyke, 1976). Porosity changes and inferred lake levels are from Benson (1988). The solid line is constrained fairly well by radiocarbon and correlated tephra ages, and by sedimentological data (fig. 10); the dashed line is poorly constrained and mostly hypothetical except where age control is available.

Figure 1

Albers Equal Area Projection

SCALE 1:7,500,000

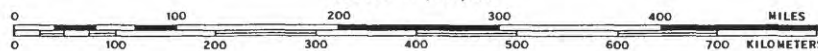


Figure 1. Sites in the western conterminous United States where age control for sediments of Walker Lake is obtained by means of tephra correlation. Map base is from U.S. Geological Survey shaded relief map, scale 1:7,500,000.

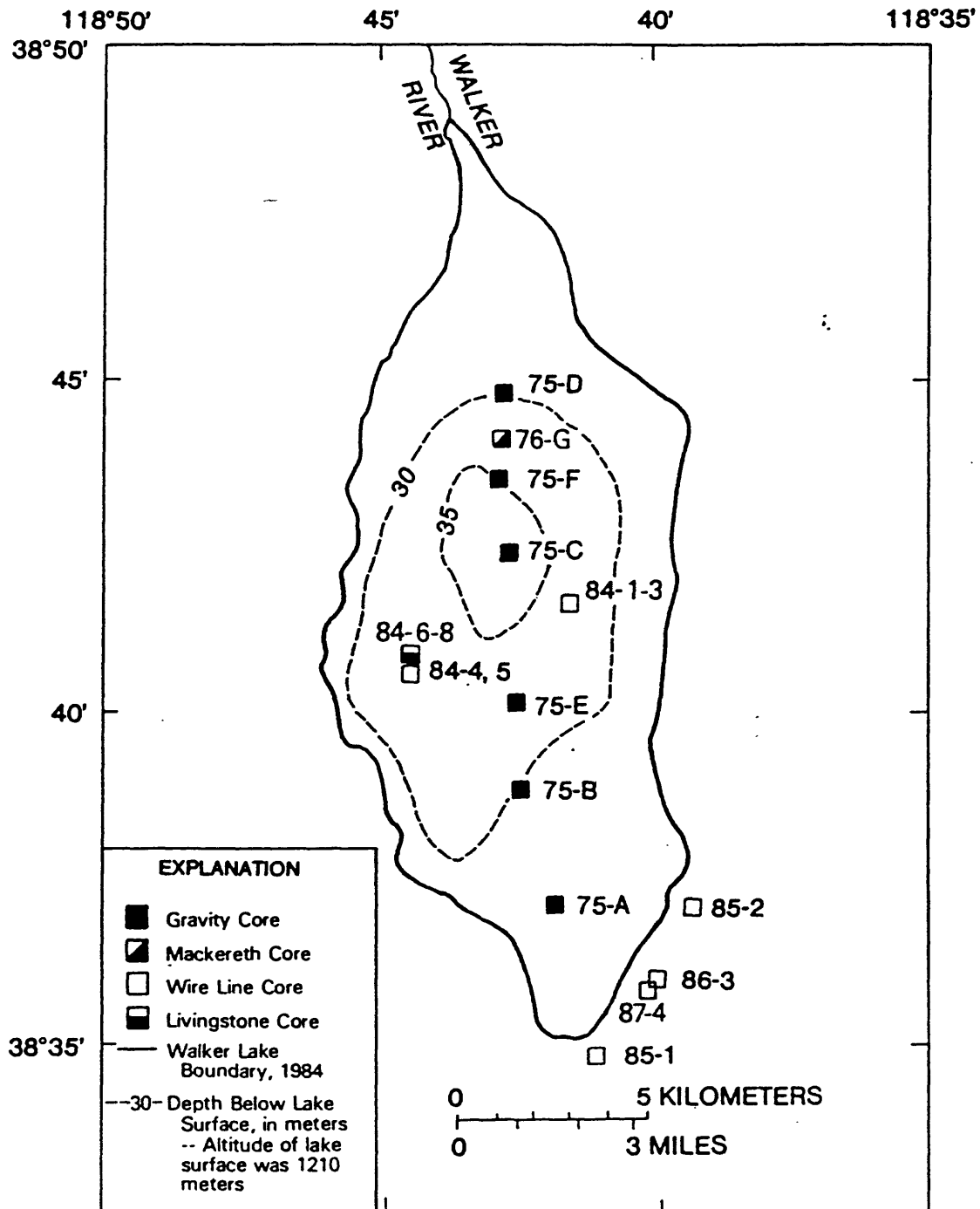


Figure 2. Location of offshore and onshore cores collected at Walker Lake. Prefix WLC omitted from core numbers. (From Benson, 1988).

119° 15'

119° 00'

118° 45'

38° 00'

37° 45'

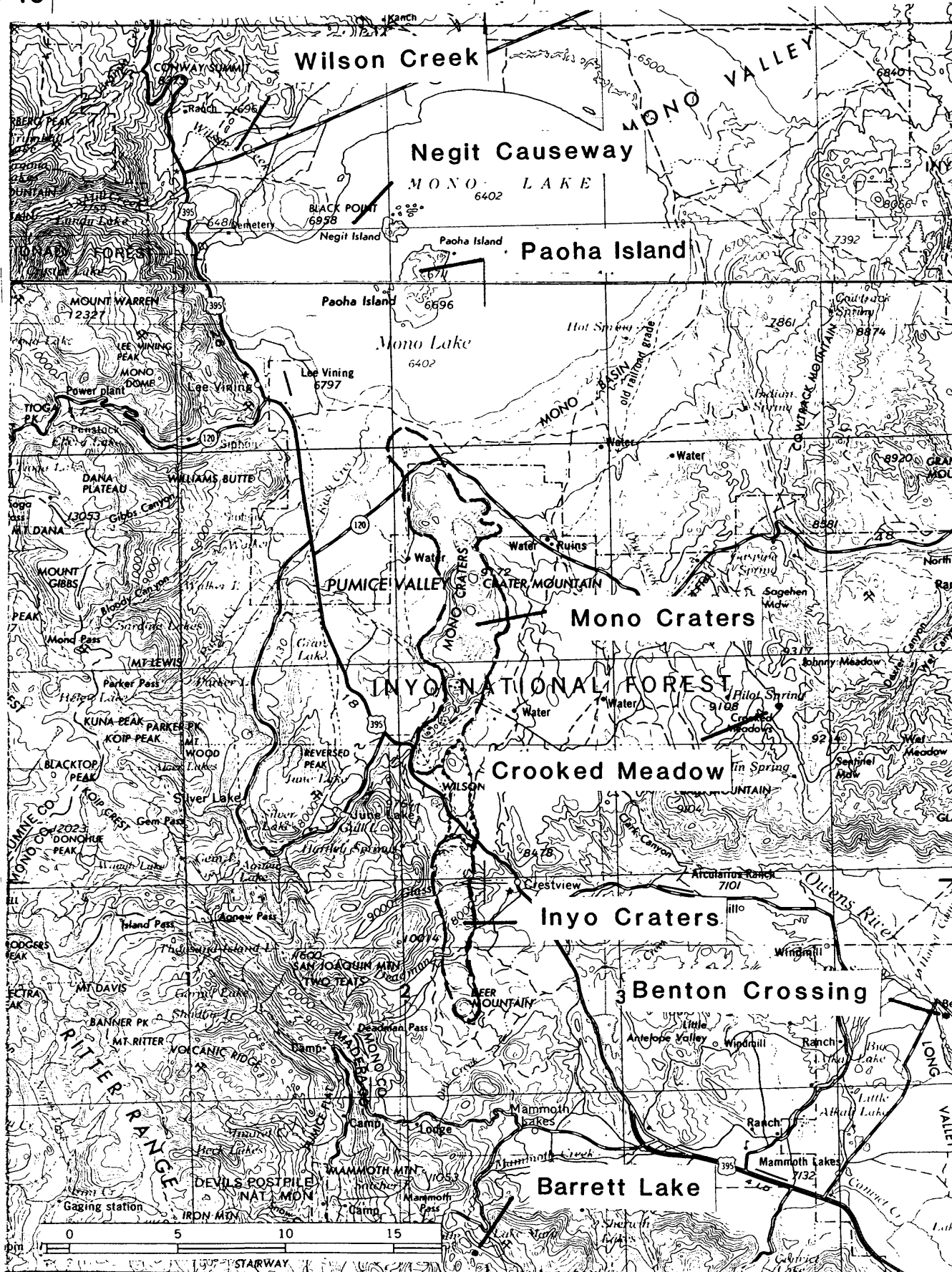


Figure 3. Location of cores and exposures south of Walker Lake where tephra layers are found that correlate with those in Walker Lake.

FIGURE 7. 1

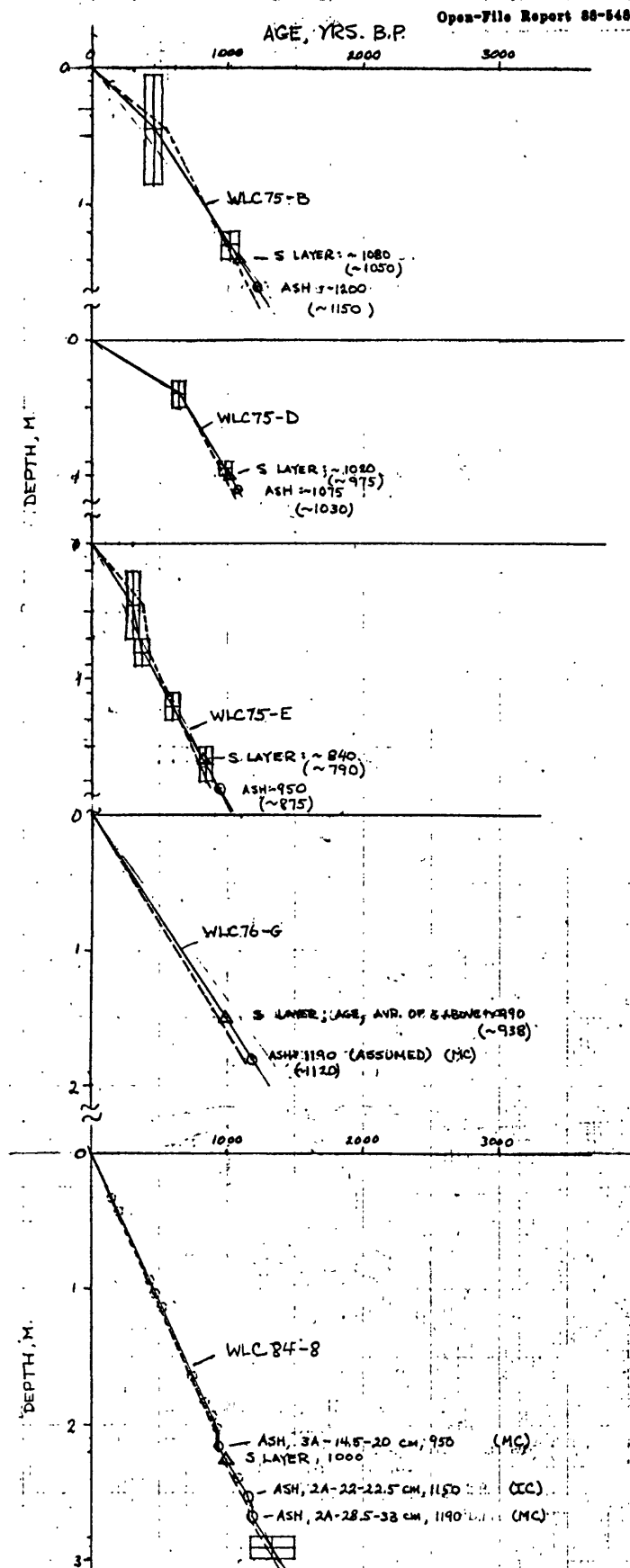
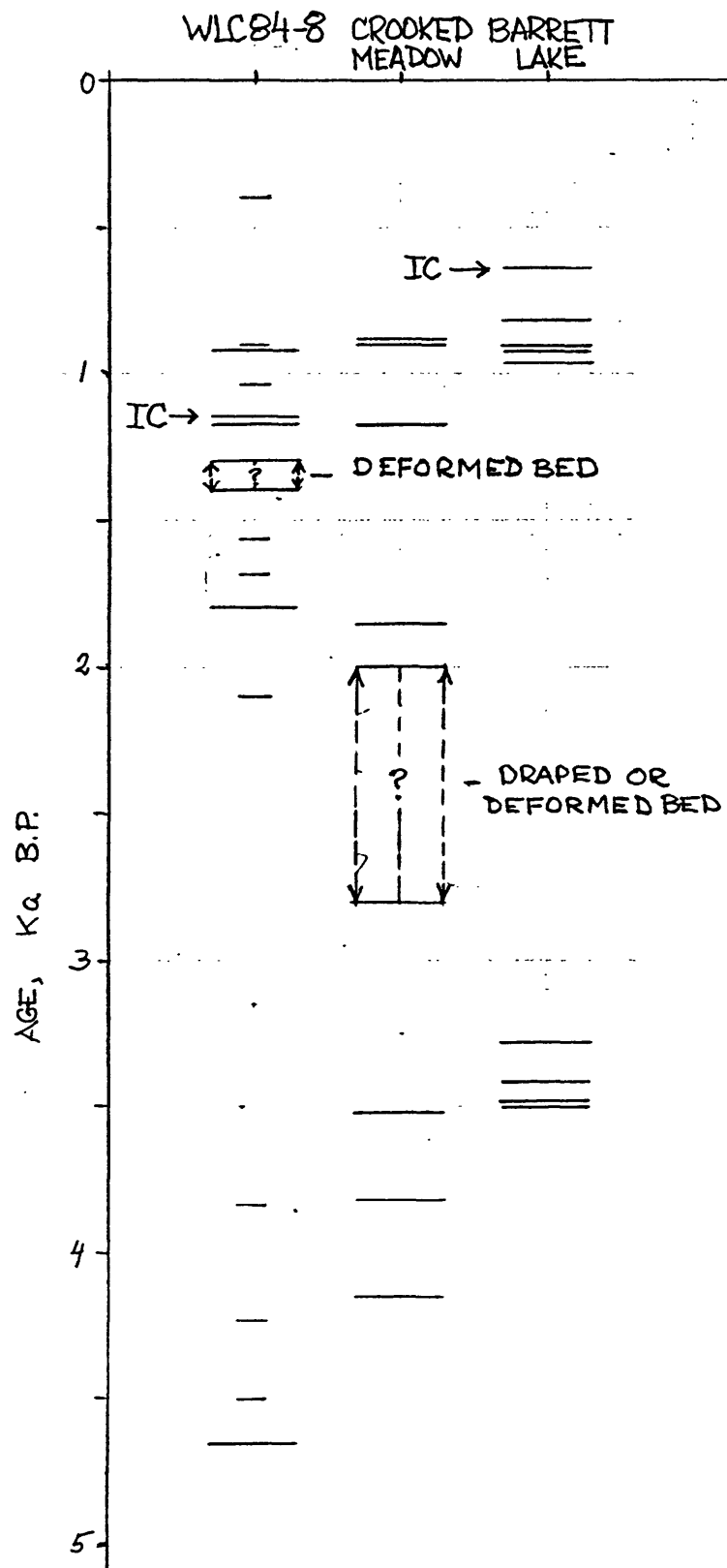


Figure 8.



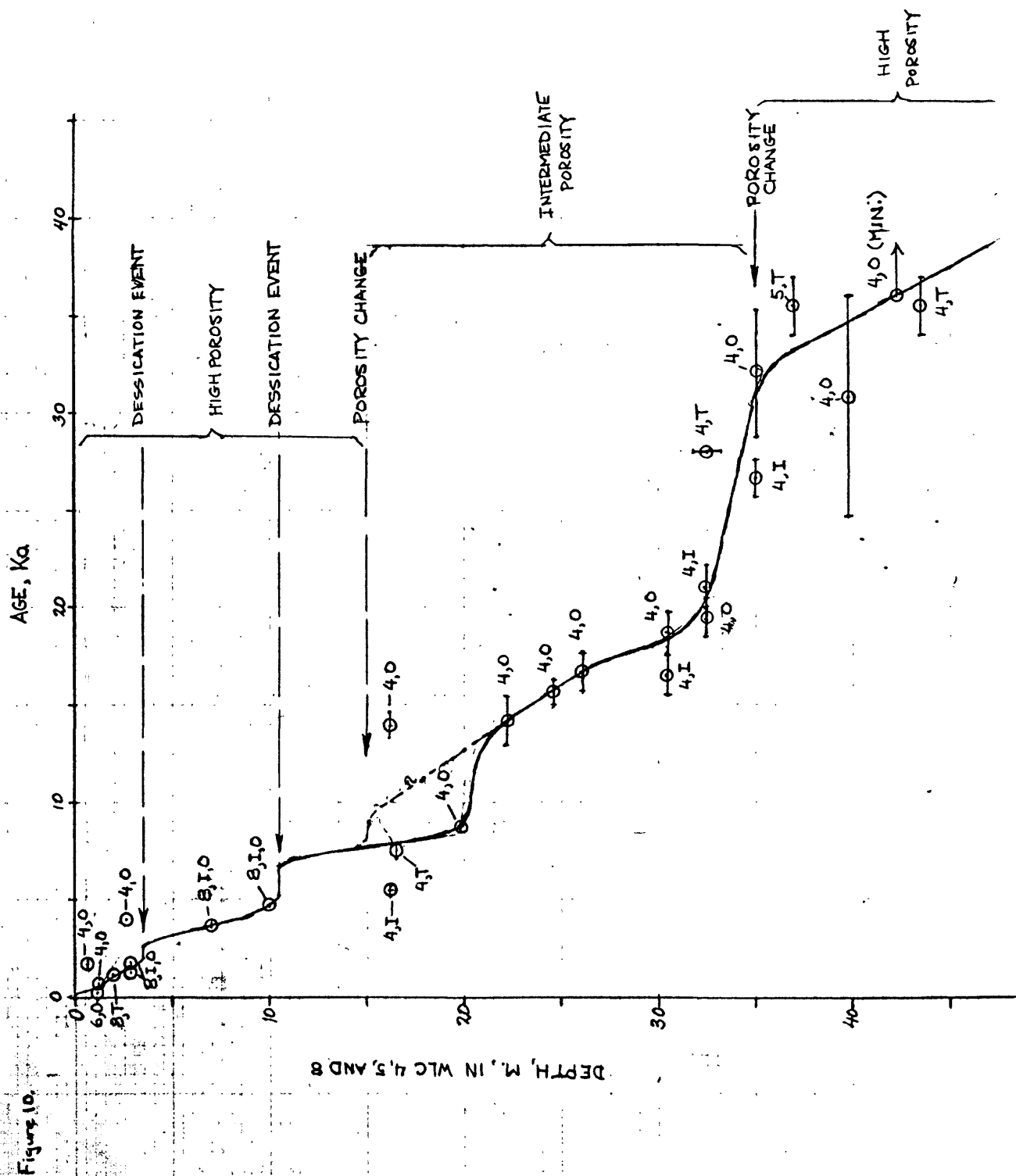


Figure 11.

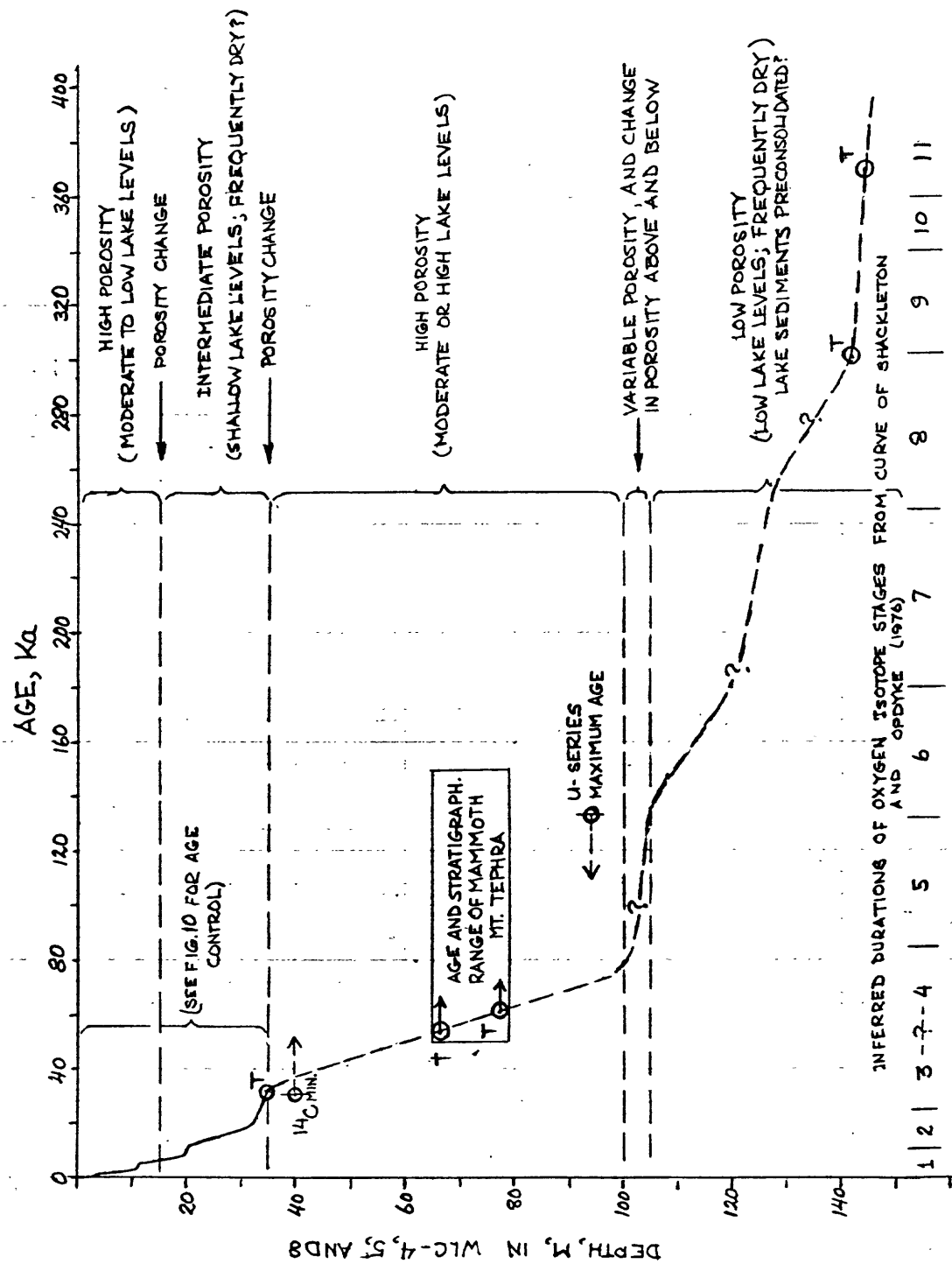


Table 2. Ages of young tephra layers in cores from Walker and Barrett Lake, and Crooked Meadow, eastern California and western Nevada. Ages are estimated from sedimentation-rate curves based on radiocarbon analyses by Yang (1988), S. R. Robinson (USGS, Menlo Park), and R. S. Anderson (Univ. of Arizona). Tephra layers were erupted from Mono Craters, California, except those Marked "IC", which were erupted from the Inyo Craters. Depths and age estimates given in parentheses are for zones of disseminated glass shards in Walker Lake core 8.

<u>Walker Lake Core 8</u>		<u>Crooked Meadow</u>		<u>Barrett Lake</u>	
Depth (m)	Est. age. (yr. BP)	Depth (m)	Est. age (yr. BP)	Depth (m)	Est. age (yr. BP)
(0.93)	(430)	---	---	---	---
---	---	---	---	0.25	640 [600] ¹ (IC)
(2.04)	(900)	0.20	880	0.40	829 [970]
2.18	920	0.23	900	0.48	900 [1110]
(2.34)	(1040)	---	---	0.51	920 [1160]
2.55)	1150 (IC)	---	---	---	---
2.67	1190	0.35	1180	0.54	960 [1200]
2.95-3.04	1300-1400 ²	---	---	---	---
(3.27)	(1570)	---	---	---	---
(3.46)	(1680)	---	---	---	---
3.68	1800	---	---	---	---
(4.09)	(2100)	0.44	1850	---	---
---	---	0.55-0.70	2000-2800 ²	---	---
---	---	---	---	1.09	3280
---	---	---	---	1.13	3420
---	---	---	---	1.15	3480
---	---	0.80	3520	1.18	3500
(7.98)	(3840)	1.00	3820	---	---
(8.99)	(4230)	1.10	4150	---	---
(9.70)	(4500)	---	---	---	---
10.15	4650	---	---	---	---
---	---	1.42	7140	---	---
---	---	2.20	10100	---	---

¹Ages in brackets represent estimates adjusted to make tephra set at 0.40-0.54 m in Barrett Lake core equivalent in age to Wood's (1977) tephra layer 2.

²Deformed or draped tephra layer; estimate of age range is based on highest and lowest positions of base of tephra layer.

Table 3. Radiocarbon ages used in estimating ages of tephra layers in Walker Lake cores. Ages are from Yang, 1988. Late Holocene ages have been also recalculated to correct for atmospheric variation of ^{14}C in the atmosphere (Stuiver and Becker, 1986; Stuiver and Reimer, 1986). na - not applicable.

Lab. Number	Segment Number	Material	Depth (m)	Age (yr. B.P.)	Error (\pm yr.)	Recalc. Age (A.D. or B.C.)	Error (\pm yr)	Recalc. Age (yr. B.P.)
Core WLC84-4								
DE-350	2	Organic	0.60- 0.69	1,600	190	435 A.D.	200	1515
DE-351	3	Organic	1.05- 1.12	600	160	1355 A.D.	120	595
DE-351	3	Organic	1.10- 1.18	550	150	550 A.D.	150	1400
DE-353	5	Organic	2.68- 2.75	4,000	280	2530 B.C.	380	4480
DE-354	7	Inorganic	16.04-16.17	5,400	250	4240 B.C.	270	6190
		Organic		14,000	730	na		
DE-368	8	Organic	19.65-19.80	8,700	310	na		
DE-355	9	Organic	22.35-22.45	14,200	1300	na		
DE-356	10	Organic	24.60-24.67	15,700	680	na		
DE-357	11	Organic	26.16-26.24	16,800	1000	na		
DE-358	12	Inorganic	30.41-30.62	16,500	1000	na		
		Organic		18,700	1100	na		
DE-359	13	Inorganic	32.48-32.62	19,500	1000	na		
		Organic		21,000	1100	na		
DE-360	14	Inorganic	35.09-35.18	26,700	1100	na		
		Organic		32,100	3900	na		
DE-364	16	Inorganic	36.20-36.32	24,000	1300	na		
		Organic		>29,960		na		
DE-361	16	Organic	39.91-39.98	30,900	6000	na		
DE-362	17	Inorganic	42.36-42.43	24,900	1900	na		
		Organic		>36,100		na		
DE-363	19	Organic	44.81-44.88	>33,700		na		
Core WLC84-5								
DE-364	5	Inorganic	36.20-35.32	24,000	1300	na		
		Organic		>29,960		na		
DE-365	6	Organic	39.71-39.83	31,400	8400	na		
Core WLC84-6								
DE-366	1	Inorganic	1.00- 1.15	350	100	1550 A.D.	135	400
		Organic		360	170	1555 A.D.	180	395
Core WLC84-8								
DE-367	2A	Inorganic	2.83- 2.99	1,700	180	330 A.D.	200	1620
		Organic		1,300	170	730 A.D.	170	1220
DE-372	2B	Inorganic	4.23- 4.39	1,900	170	95 A.D.	205	1855
		Organic		2,600	170	760 B.C.	170	2710
DE-370	4	Inorganic	6.92- 7.07	3,800	200	2260 B.C.	280	4210
		Organic		3,800	200	2260 B.C.	280	4210
DE-371	8	Inorganic	10.00-10.24	4,700	220	3460 B.C.	280	5410
		Organic		4,700	220	3460 B.C.	280	5410
DE-369	9	Inorganic	10.90-11.15	4,700	230	3450 B.C.	290	5400
		Organic		4,700	110	3475 B.C.	145	5425

Table 5. Electron-microprobe (EM), energy-dispersive X-ray fluorescence (XRF), and instrumental neutron activation (INA) analyses of some tephra layers from Walker Lake cores, and tephra layers of similar chemical composition from other sites. Samples labelled WLC are from cores in Walker Lake; samples labelled KRL are from the Negit Island causeway (in stratigraphic sequence, with II-3 at the top, and II-8 at the base), and sample KDP 73-140 is a rhyodacite from Mammoth Mountain, in Long Valley, erupted during an interval ca. 50-150 Ka B.P. (Bailey and others, 1976). All analyses are of volcanic glass separated from the tephra, except for KDP 73-140, which is of whole-rock. n.d. - not determined. Analysts: C. E. Meyer, U.S.G.S., Menlo Park, CA (EM), J. L. Slate, U.S.G.S., Menlo Park, CA (XRF), and J. Budahn, D. Knight, and D. McKown, U.S.G.S., Lakewood, CO (INA).

Element or Oxide	Samples								
	WLC84-5 (64.51m)	WLC84-5 (78.91m)	WLC84-4 (78.77m)	WLC84-3 (38.26m)	KRL71082 II-3	KRL71082 II-4	KRL71082 II-5	KRL71082 II-8	KDP-73-140 (whole-rock) ²
Electron Microprobe Analysis (Major and Minor elements)									
SiO ₂ , %	77.18	77.29	77.12	76.22	72.65	76.44	72.51	76.09	70.55
Al ₂ O ₃ , %	12.84	12.54	12.57	13.30	14.86	13.18	14.72	13.39	15.77
Fe ₂ O ₃ , %	0.88	0.79	0.89	0.89	1.27	0.88	1.33	0.90	1.67
MgO, %	0.04	0.06	0.08	0.10	0.12	0.05	0.15	0.08	0.26
MnO, %	0.06	0.05	0.04	0.03	n.d.	n.d.	n.d.	0.03	0.12
CaO, %	0.73	0.84	0.86	0.83	0.49	0.70	0.59	0.83	0.77
TiO ₂ , %	0.07	0.08	0.11	0.10	0.24	0.07	0.29	0.09	0.33
Na ₂ O, %	3.53	3.62	3.50	3.61	5.26	3.69	5.03	3.74	5.68
K ₂ O, %	4.78	4.73	4.83	4.92	5.11	4.98	5.38	4.85	4.79
Total, % (orig.) ¹	94.66	95.11	95.48	95.22	94.11	96.11	96.78	96.05	96.68
Energy-dispersive X-ray Fluorescence Analysis (Major, Minor, and Trace Elements)									
K ₂ O, %	4.80	4.89	5.04	5.00	5.41	5.17	5.31	5.01	4.79
CaO, %	0.76	0.82	0.85	0.87	0.60	0.79	0.69	0.88	0.77
TiO ₂ , %	0.064	0.088	0.106	0.110	0.229	0.069	0.272	0.105	0.33
MnO, %	0.050	0.051	0.049	0.049	0.141	0.053	0.116	0.051	0.12
Fe ₂ O ₃ , %	0.90	0.86	0.93	0.93	1.34	0.94	1.40	0.93	1.67
Rb, ppm	184	171	167	162	120	183	126	165	n.d.
Sr, ppm	42	83	107	106	13	40	41	107	140
Y, ppm	15	14	11	11	30	12	28	15	29
Zr, ppm	78	82	90	94	312	77	314	93	419
Nb, ppm	13	14	11	11	25	11	23	11	n.d.
Neutron Activation Analysis (Major, Minor, and Trace Elements)									
Sc, ppm	1.80	1.75	1.67	1.63	3.58	1.69	3.47	1.67	3.84
Mn, ppm	349	333	323	316	793	329	699	312	920
Fe, %	0.61	0.56	0.61	0.58	0.84	0.59	0.92	0.63	1.24
Zn, ppm	34	37	38	35	67	72	64	31	58
Rb, ppm	168	154	158	145	106	163	113	157	116
Cs, ppm	5.10	4.75	4.42	4.15	2.28	4.76	2.54	4.43	1.5
Ba, ppm	166	404	654	601	696	178	1030	672	1644
La, ppm	17	21	27	26	59	17	58	28	72
Ce, ppm	35	39	47	45	121	31	120	50	128
Nd, ppm	13	14	16	15	44	11	42	17	51
Sm, ppm	3.03	2.87	3.06	2.92	7.52	2.88	7.23	3.13	8.7
Eu, ppm	0.26	0.31	0.36	0.33	0.92	0.25	1.09	0.38	1.4
Tb, ppm	0.42	0.38	0.37	0.34	0.82	0.41	0.82	0.37	0.86
Dy, ppm	2.8	2.5	2.4	2.4	5.6	2.8	5.2	2.2	n.d.
Yb, ppm	1.78	1.54	1.51	1.39	3.21	1.78	3.26	1.43	3.6
Lu, ppm	0.26	0.23	0.21	0.20	0.48	0.24	0.47	0.22	0.48
Hf, ppm	3.37	3.11	3.18	3.11	8.48	3.16	8.41	3.08	9.9
Ta, ppm	1.83	1.66	1.59	1.43	1.89	1.66	1.84	1.53	1.91
Th, ppm	17.6	15.5	16.2	14.9	10.9	16.2	11.4	16.0	10.7
U, ppm	5.6	4.8	4.6	4.3	3.3	5.0	3.5	4.6	3.3

¹Original total before oxide percentages were recalculated to 100 percent. Most of the deficit observed between the original totals and 100 percent is due to the presence of water of hydration and other fluids that are present in the glass.

²Data from R. A. Bailey, U.S.G.S., Menlo Park, CA, written commun., 1988.

Table 6. Electron microprobe (EM), energy-dispersive X-ray fluorescence (XRF), and instrumental neutron-activation analyses (INA) of a tephra layer from the lower part of core WLC84-5 in Walker Lake, of tephra layers of similar chemical composition, and of stratigraphically related tephra layers from other sites in the region. WLC - sample of tephra layer from core in Walker Lake; PAOH - tephra layers from Paoha Island, Mono Lake, CA (in stratigraphic sequence, with PAOH-1 at top and PAOH-2 at the base); KRL and M - tephra layers from Benton Crossing, Long Valley, CA (in stratigraphic sequence, with KRL10779A at top and M7811 at the base). Analysts as in tables 4 and 5.

Element	Samples						
or Oxide	WLC 84-5-42A (141.78m)	Paoha Island PAOH-3	PAOH-1	PAOH-2	Benton Crossing KRL10779A	M7810	M7811
Electron-Microprobe Analysis (Major and Minor Elements)							
SiO ₂ , %	74.35	72.80	72.87	69.14	73.31	73.36	69.23
Al ₂ O ₃ , %	13.74	14.98	14.91	15.06	14.49	14.56	15.14
Fe ₂ O ₃ , %	2.30	2.20	2.28	3.84	2.27	2.19	3.88
MgO, %	0.18	0.40	0.15	0.67	0.43	0.44	0.69
MnO, %	0.06	0.03	0.07	0.08	0.04	0.03	0.10
CaO, %	1.04	2.08	1.00	2.22	2.11	2.08	2.28
TiO ₂ , %	0.20	0.27	0.19	0.70	0.30	0.26	0.66
Na ₂ O, %	5.18	4.24	5.56	5.43	4.06	4.03	5.15
K ₂ O, %	2.94	3.00	2.97	2.86	3.00	3.05	2.86
Total (orig.) ¹	93.27	94.77	94.51	96.14	95.99	94.93	96.36
Energy-dispersive X-ray Fluorescence Analysis (Major, Minor, and Trace Elements)							
K ₂ O, %	3.00	3.06	3.40	2.84	3.02	4.88	2.80
CaO, %	0.91	1.91	0.92	1.95	1.88	0.92	1.96
TiO ₂ , %	0.188	0.260	0.184	0.553	0.261	0.206	0.548
MnO ₂ , %	0.077	0.046	0.079	0.116	0.049	0.038	0.120
Fe ₂ O ₃ , %	2.22	2.33	2.32	3.92	2.28	1.02	3.97
Rb, ppm	74	97	80	81	99	166	78
Sr, ppm	74	265	83	201	270	98	197
Y, ppm	28	10	31	41	10	11	36
Zr, ppm	238	168	269	281	173	111	277
Nb, ppm	9	5	10	12	4	7	11
Instrumental Neutron Activation Analysis (Major, Minor, and Trace Elements)							
Sc, ppm	n.d.	3.22	4.80	9.67	2.98	1.41	9.80
Mn, ppm	n.d.	291	494	711	288	257	711
Fe, %	n.d.	1.56	1.56	2.69	1.55	0.67	2.66
Zn, ppm	n.d.	47	72	75	44	n.d.	73
Rb, ppm	n.d.	82	68	71	86	163	69
Cs, ppm	n.d.	6.19	3.26	3.38	6.30	8.9	3.57
Ba, ppm	n.d.	652	767	851	692	959	825
La, ppm	n.d.	18	25	25	19	24	25
Ce, ppm	n.d.	38	54	55	37	45	53
Nd, ppm	n.d.	14	23	27	14	13	26
Sm, ppm	n.d.	2.69	2.63	6.61	2.95	2.12	6.66
Eu, ppm	n.d.	0.57	0.81	1.35	0.55	0.33	1.32
Tb, ppm	n.d.	0.33	0.88	1.10	0.32	0.28	1.03
Dy, ppm	n.d.	n.d.	6.0	7.3	2.1	1.9	6.2
Yb, ppm	n.d.	1.34	3.87	4.47	1.39	1.64	4.30
Lu, ppm	n.d.	0.21	0.57	0.66	0.21	0.24	0.64
Hf, ppm	n.d.	4.86	7.38	7.56	5.01	3.60	7.57
Ta, ppm	n.d.	0.67	1.07	1.13	0.67	0.71	1.11
Th, ppm	n.d.	9.1	6.5	7.0	9.7	20.7	7.0
U, ppm	n.d.	3.7	2.4	2.7	4.2	6.3	2.6

¹Original total before oxide percentages were recalculated to 100 percent. Most of the deficit observed between the original totals and 100 percent is due to the presence of water of hydration and other fluids that are present in the glass.